ELSEVIER

Contents lists available at ScienceDirect

Brain Behavior and Immunity

journal homepage: www.elsevier.com/locate/ybrbi





Repeated social defeat stress differently affects arthritis-associated hypersensitivity in male and female mice

Carmen La Porta^{a,*}, Thomas Plum^b, Rupert Palme^c, Matthias Mack^d, Anke Tappe-Theodor^{a,*}

- a Institute of Pharmacology, Medical Faculty Heidelberg, Heidelberg University, Im Neuenheimer Feld 366, 69120 Heidelberg, Germany
- ^b Division for Cellular Immunology, German Cancer Research Center, Im Neuenheimer Feld 280, 69120 Heidelberg, Germany
- ^c Department of Biomedical Sciences, University of Veterinary Medicine, Vienna, Austria
- ^d Department of Nephrology, Regensburg University Hospital, Regensburg, Germany

ARTICLE INFO

Keywords: Social defeat Arthritis Pain Cytokines Monocytes Neutrophils Microglia

ABSTRACT

Chronic stress enhances the risk of neuropsychiatric disorders and contributes to the aggravation and chronicity of pain. The development of stress-associated diseases, including pain, is affected by individual vulnerability or resilience to stress, although the mechanisms remain elusive. We used the repeated social defeat stress model promoting susceptible and resilient phenotypes in male and female mice and induced knee mono-arthritis to investigate the impact of stress vulnerability on pain and immune system regulation. We analyzed different painrelated behaviors, measured blood cytokine and immune cell levels, and performed histological analyses at the knee joints and pain/stress-related brain areas. Stress susceptible male and female mice showed prolonged arthritis-associated hypersensitivity. Interestingly, hypersensitivity was exacerbated in male but not female mice. In males, stress promoted transiently increased neutrophils and Ly6Chigh monocytes, lasting longer in susceptible than resilient mice. While resilient male mice displayed persistently increased levels of the anti-inflammatory interleukin (IL)-10, susceptible mice showed increased levels of the pro-inflammatory IL-6 at the early- and IL-12 at the late arthritis stage. Although joint inflammation levels were comparable among groups, macrophage and neutrophil infiltration was higher in the synovium of susceptible mice. Notably, only susceptible male mice, but not females, presented microgliosis and monocyte infiltration in the prefrontal cortex at the late arthritis stage. Blood Ly6Chigh monocyte depletion during the early inflammatory phase abrogated late-stage hypersensitivity and the associated histological alterations in susceptible male mice.

Thus, recruitment of blood $Ly6C^{high}$ monocytes during the early arthritis phase might be a key factor mediating the persistence of arthritis pain in susceptible male mice. Alternative neuro-immune pathways that remain to be explored might be involved in females.

1. Introduction

All living individuals have to react to unforeseen stressful stimuli (Nicolaides et al., 2014). Stress is increasing worldwide, representing the leading cause of mental disorders, including depression (American Psychiatric Association (APA), 2013), which is the fifth leading cause of years lived with disability (Vos et al., 2017). Importantly, stress affects each individual differently, depending on the genetic, epigenetic, and constitutional vulnerability or resilience (Cathomas et al., 2019).

The stress response is mediated by the autonomic nervous system and the hypothalamus–pituitary–adrenal axis (HPAA), which induce the secretion of (nor)adrenaline and cortisol (corticosterone in rodents),

respectively (Cathomas et al., 2019; Sawicki et al., 2020; Weber et al., 2017; Wohleb et al., 2015), regulating the immune system as a physiological response to maintain homeostasis (Ader et al., 1995; Cathomas et al., 2019; Wohleb et al., 2015). Excessive or prolonged stress induces elevated peripheral levels of cytokines (i.e., IL-6) and immune cells (i.e., monocytes and neutrophils), which have been associated with mental disorders, like anxiety and depression (Cathomas et al., 2019; Raison et al., 2006; Weber et al., 2017), and also contribute to the chronicity and exacerbation of different inflammatory diseases, including arthritis (Davis et al., 2009; Sawicki et al., 2020; Straub et al., 2005).

Arthritis is one of the most prevalent chronic health problems for which osteoarthritis is the most common form (Hunter and Bierma-

E-mail addresses: carmen.laporta@pharma.uni-heidelberg.de (C. La Porta), anke.tappe-theodor@pharma.uni-heidelberg.de (A. Tappe-Theodor).

https://doi.org/10.1016/j.bbi.2024.04.025

^{*} Corresponding authors.

Zeinstra, 2019). The main symptoms are pain and disability, associated with articular cartilage damage, bone remodeling, and recurrent synovial inflammation (Geyer and Schönfeld, 2018; Hunter and Bierma-Zeinstra, 2019; Yu et al., 2022). Local and systemic inflammation is increasingly recognized to be involved in joint pathological changes (Cremers et al., 2017) and the associated pain (Dainese et al., 2022), with a crucial role of neutrophils, macrophages and monocytes releasing pro-inflammatory factors (Bai et al., 2022; Chaney et al., 2022; Cremers et al., 2017; Dainese et al., 2022; Geraghty et al., 2021; Hsueh et al., 2021; Mathiessen and Conaghan, 2017; Smolen and Steiner, 2003; Valdrighi et al., 2022). Moreover, peripheral inflammatory signals also propagate to the central nervous system (CNS) via the interaction of circulating cytokines and leukocytes with microglia and perivascular macrophages (Malange et al., 2022), leading to neuroinflammation, which is involved in pain regulation and comorbid anxiety and depression (Harth and Nielson, 2019; Malange et al., 2022; Setiawan et al., 2015).

Arthritis progression varies considerably among individuals, depending on immune and psychosocial factors (Davis et al., 2009; Uhlig et al., 2000). Stress resilience appears to have a protective role and is associated with lower pain and disability (Johnson et al., 2019; Sturgeon et al., 2016; Sturgeon and Zautra, 2010). Therefore, it is important to consider individual vulnerability and investigate the potential mechanisms that distinguish resilience and susceptibility to achieve better treatment strategies.

This study aimed to investigate the impact of chronic stress on pain and the immune response in the mouse model of kaolin/carrageenan (K/C)- induced arthritis. We used the repeated social defeat stress (RSDS) model (Golden et al., 2011; Harris et al., 2018) to assess the effect of vulnerability and resilience to stress in male and female mice. We studied its impact on diverse pain-related behaviors and histological alterations induced by the arthritis model. Furthermore, we analyzed associated immune cell and cytokine profiles in the blood and synovial fluid and neuroinflammatory markers in the brain.

2. Materials and methods

2.1. Animals and housing conditions

We used 8-week-old C57BL/6J male and female mice and >4-month-old retired CD-1 male breeders (Charles River, Germany) at the beginning of the experiments. Mice were housed in individually ventilated cages (IVC) green line GM500 (391 \times 199 \times 160 mm, floor area 501 cm2) connected to a ventilation system (Tecniplast). Upon delivery, C57BL/6J mice were housed in groups of 4 before repeated social defeat stress (RSDS) and 2 per cage after RSDS until sacrifice. CD-1 mice were singly housed before and after RSDS. They had ad libitum access to food and water under a 12-hour light/ dark cycle (7:00 am/ 7:00 pm), ambient temperature (22 \pm 2 $^{\circ}$ C), and humidity (40—60 %). The general health of mice was checked daily. Animal housing rooms were on the same floor, close to the behavioral rooms.

All procedures followed the ethical guidelines imposed by the local governing body (Regierungspräsidium Karlsruhe, Germany; file no. 35–9185.81/G-240/19) and the International Association for the Study of Pain (IASP) guidelines for animal pain research. Animal experiments complied with the ARRIVE guidelines and have been conducted in accordance with the EU Directive 2010/63/EU for animal experiments. All efforts were made to minimize animal suffering and reduce the number of animals used. Experimenters were blind to group assignments and outcome assignments and mice were randomly assigned to the different groups.

2.2. Repeated social defeat stress (RSDS) model

RSDS was performed as previously described in male (Golden et al., 2011) and female mice (Harris et al., 2018). One day before RSDS

started, previously selected CD-1 aggressor mice (Golden et al., 2011) were singly housed on one side of a cage equipped with a clear perforated Plexiglas divider in the middle. Experimental C57BL/6J mice were exposed every day for ten consecutive days to a novel CD-1 aggressor in its home cage for up to five minutes of physical aggression and immediately after were placed on the opposite side of the perforated divider, allowing for physical separation but continuous sensory contact with the aggressor for 24 h. The social defeat session lasted up to 5 min, during which mice were carefully observed. The session was terminated before the 5 min had expired if the defeated mice started to be severely wounded. Male and female mice were exposed to the same RSDS procedure, except that we applied male urine to female mice (20 μ l at the base of the tail and vaginal orifice) immediately before each daily RSDS session to induce repetitive attacks from aggressive male CD1 mice (Harris et al., 2018). Mice were visually inspected for wounding, and mice with excessive wounding or moribund were immediately

Control mice were housed in two per cage in identically partitioned cages and rotated daily within the other controls' cages to simulate the defeated mice's rotation with the new aggressors. On the day of the last defeat bout, experimental defeated mice were also housed in two per cage and separated by the divider till the end of the experiments.

2.3. Knee joint mono-arthritis model

Knee mono-arthritis was induced as previously described (Tappe-Theodor et al., 2011). Mice were anesthetized with a sleep-mix solution composed of Fentanyl (0.01 mg/kg; Janssen-Cilag, Germany), Medeto-midine (0.3 mg/kg; Alvetra, Germany) and Midazolam (4 mg/kg; Hameln Pharma Plus, Germany). Kaolin (Sigma, Germany) suspension (4 %, 40 μ l) was slowly injected into the joint cavity through the patellar ligament of the right knee. After repetitive flexions and extensions of the hindlimb for 15 min, a carrageenan (Sigma) solution (2 %, 40 μ l) was injected into the same knee joint and flexed and extended for another 5 min. The control group of mice received saline solution. The anesthesia was antagonized with i.p. injection of Naloxone (0.4 mg/kg; Inresa Arzneimittel, Germany), Flumazenil (0.5 mg/kg; Fresenius, Germany), and Atipamezole (2.5 mg/kg; Prodivet Pharmaceuticals, Belgium).

2.4. Antibody treatment for monocyte depletion

Male C57BL/6J mice with K/C-induced arthritis received daily i.p. injections of a rat anti-mouse C-C motif chemokine receptor (CCR2) monoclonal antibody (clone MC-21, provided by Prof. Matthias Mack), or IgG2b kappa isotype control (clone LTF-2, BioXCell, Germany) (Brühl et al., 2007; Mack et al., 2001; Pfau et al., 2019). Antibodies were administered at a dose of 20 μ g per mouse per day in 100 μ L of sterile phosphate buffer saline (PBS) for 5 consecutive days starting one day before mono-arthritis induction. The injection protocol lasted 5 days because after that the antibody becomes ineffective due to the generation of mouse anti-rat antibodies (Brühl et al., 2007; Pfau et al., 2019).

2.5. Behavioral tests

All behavioral tests were performed between 9 am and 2 pm, except for the voluntary wheel running, which was performed during the active time. Mice were brought into the behavioral room half an hour before behavioral testing.

2.5.1. Social interaction (SI) test

SI test was performed as described previously (Golden et al., 2011). In the first phase of the test (no target phase), defeated mice were placed in an open-field arena with an empty cylindrical wire enclosure placed at one end and centered against the wall, and mouse exploratory behavior was tracked for 150 s in the absence of the target CD-1 mouse using Sygnis Tracker software (Sygnis, Germany).

In the second phase (target phase), a non-familiar CD-1 mouse was placed in the enclosure. Exploratory behavior of the defeated mouse was recorded for additional $150 \, \text{s}$.

SI ratio and time spent in interaction and corner zones of the arena were calculated. The SI ratio was obtained by dividing the time spent in the interaction zone when the target is present by the time spent in the interaction zone when the target is absent. A SI ratio equal to 1 was used as the threshold for dividing defeated mice into susceptible and resilient.

2.5.2. Anxiety-like behavior

2.5.2.1. Elevated plus maze (EPM) test. The EPM test was performed as previously described (La Porta and Tappe-Theodor, 2020). The mice were placed in the center of the maze facing the closed arms, and five-minute test sessions were digitally recorded with Sygnis Tracker software (Sygnis, Heidelberg, Germany) to measure the time spent in each

2.5.2.2. Elevated zero maze (EZM) test. The EZM apparatus (Ugo Basile, Varese, Italy) consisted of a circular maze (50 cm diameter, 5 cm track width) with 50 % enclosed (20 cm wall height) and 50 % open areas. Mice were placed in the open space facing the closed area. The time and distance exploring the two arena compartments were recorded with the Sygnis Tracker for 5 min, as previously described (Elkhatib et al., 2020).

2.5.3. Anhedonic-like behavior - sucrose preference (SP) test

Anhedonia was measured with the SP test, as previously described (Menard et al., 2017). This test was performed in the home cage equipped with the separator containing two mice (one per side) by removing the standard water bottles and replacing them with two drinking bottles per mouse (50 mL Falcon® with siliconized rubber stops and stainless steel sipper tubes). The two bottles were filled with water for a 24-h habituation period. Next, water from one bottle was replaced with a 1 % sucrose solution, and mice were allowed to drink ad libitum for 24-h hours. These first 24 h of sucrose availability were used as another habituation period, as the non-familiar sucrose solution could induce neophobia. Subsequently, the side of the bottles was switched for an additional 24-h period of drinking to prevent place preference. The amount of water and sucrose solution consumed by each mouse was measured daily by weighing the bottles. At the end of the 48-h testing, sucrose preference was calculated by dividing the total amount of sucrose solution consumed by the total amount of liquid (water plus sucrose solution) consumed over the last 24 h.

2.5.4. Depressive-like behavior - tail suspension (TS) test

The TS test was performed as previously described (La Porta and Tappe-Theodor, 2020). Mice were suspended by their tail with adhesive tape 50 cm above the surface, and the immobility time was recorded and manually analyzed during the whole testing period of 6 min.

2.5.5. Mechanical sensitivity - von Frey (vF) test

Mice were kept in standard plastic modular enclosures on top of a perforated metal platform (Ugo Basile, Varese, Italy), enabling the application of von Frey filaments (North Coast Medical, Gilroy, CA, USA) to the center of the plantar surface of the mouse paw from below. Mice were acclimatized on three consecutive days for one h to the von Frey compartments and at least 30 min before starting the measurements on each experimental day. Filaments with increasing forces of 0.07, 0.16, 0.4, 0.6, 1, and 1.4 g were consecutively applied to the plantar surface center of both hindpaws until bending. Each filament was tested five times on each paw with a minimum two-minute resting interval between each application, and the number of withdrawals was recorded. Mechanical sensitivity was expressed as a 60 % response threshold (g), defined as the minimum pressure required for eliciting 60 % of withdrawal responses out of five stimulations or as % of response

frequency to each filament, as previously described (La Porta and Tappe-Theodor, 2020).

2.5.6. Heat sensitivity - plantar test

Heat sensitivity was assessed by evaluating the hindpaw withdrawal latency in response to radiant heat with the Hargreaves apparatus (Ugo Basile, Varese, Italy), as previously shown (La Porta and Tappe-Theodor, 2020). Mice were kept in standard plastic modular enclosures on top of a glass platform, enabling the application of the radiant heat source (infrared intensity 50) to the hindpaw plantar surface. Mice were acclimatized on three consecutive days for one h to the setup and at least 30 min before starting the measurements on each experimental day.

The withdrawal latency was calculated by averaging three measures on each paw with a minimum of five minutes resting interval and a cutoff time of 20 s.

2.5.7. Gait analysis

The CatWalk XT system (10.6 version) (Noldus, Wageningen, The Netherlands) assessed static and dynamic gait parameters. The apparatus consists of an enclosed black corridor (1.3 m long) on a glass plate, internally illuminated with a green LED light. The mouse is placed at one end of the corridor and allowed to pass through it. The Illuminated footprintsTM technology captured the paw prints when the mice walked from one side to the other of the apparatus corridor, and the CatWalk XT software calculated statistics related to print dimensions and time and distance relationships between footfalls.

Mice were habituated to the CatWalk setup and allowed to cross the corridor during three sessions one week before starting the experiments. On each testing day, mice were allowed to cross the corridor three times. Only completed trials within the defined speed range between 10 and 20 cm/s, with a speed variance < 60 %, were accepted as passed runs and included in the analysis. Three passed runs for each mouse were semi-automatically analyzed for one selected static (stand time) and one dynamic (swing time) gait parameter. To better illustrate pain-associated changes in these parameters, run data of the right (RH) and left (LH) hind paw were displayed as RH/LH ratio obtained from the average of three runs per animal (Nees et al., 2023; Pitzer et al., 2016).

2.5.8. Voluntary wheel running

Free choice wheel running activity was monitored with an activity wheel chamber system (Lafayette Instrument, Louisiana, USA), as previously described (2). Mice were individually placed in cages with free access to a running wheel (diameter 12 cm, width 5.5 cm) equipped with an optical sensor to detect the total revolutions of the wheel and connected to a USB Interface and PC running an AWM Software (Lafayette Instrument). Mice were not trained before starting the experiments. Water and food were provided in the cage, and the running activity on the wheel was monitored from 6p.m. to 8 a.m. (14 h) on each experimental day and this period included the dark phase of the light cycle (from 7p.m. to 7 a.m.). It was chosen based on a previous study showing that mice are particularly active on the running wheel during this period compared to the light day phase (Pitzer et al., 2016).

2.6. Knee diameter

Knee diameter (in mm) was measured using a digital electronic caliper (Fine Science Tools, Heidelberg, Germany) along the anteroposterior and medio-lateral axis of the joint to assess swelling. Data were displayed as the difference (Δ) between the right and left knees.

2.7. Fecal corticosterone metabolite (FCM) measurement

FCM levels were non-invasively measured, as previously described (Segelcke et al., 2023). Feces were collected around noon by individually placing the mice in empty Macrolon Type II cages (Tecniplast) for 60 min to collect a minimum of 5–6 fecal boli and stored at $-20\,^{\circ}\text{C}$ until

extraction. Fecal samples were dried for two hours at 80 °C before mechanical homogenization, and 0.05 g were extracted with 1 ml 80 % methanol for 30 min on a vortex. After centrifugation for 10 min at 2500 g, 0.5 ml supernatant was frozen until analysis. FCMs were measured using a 5α -pregnane- 3β ,11 β ,21-triol-20-one enzyme immunoassay (Touma et al., 2003).

2.8. Blood serum collection for FACS and cytokine analysis

Blood was collected in briefly anesthetized mice via the puncture of the submandibular vein on day 12 post-SDS and day 5 and 35 post-KC. Mice were briefly anesthetized in an induction chamber with 1.5 % isoflurane in a 30 %/70 % oxygen/nitrous oxide mixture. The submandibular vein was punctured with the tip of a 25-gauge needle, allowing the blood to flow out and collect in an Eppendorf tube. Seventy-five microliter of blood were immediately transferred to a tube pre-coated with 25 ul of EDTA (1.5 mg/ml of blood) to avoid coagulation. Blood cells were then pelleted by centrifugation for 5 min at 300 g, and the supernatant (plasma) was frozen until further analysis. The remaining cell pellets were then resuspended in red blood cell lysis buffer, and lysis was performed according to the manufacturer's protocol (RBC Lysis Buffer, BioLegend). After washing with PBS supplemented with 5 % fetal calf serum (FCS, Sigma-Aldrich), cells were analyzed by flow cytometry as described below.

2.9. Synovial fluid collection for FACS and cytokine analysis

Synovial fluid was collected from the knee at day 35 post-KC immediately after euthanasia with an overdose of CO $_2$. The joint skin was excised, the patellar ligament cut below the patella and the patella was lifted to expose the synovial membrane. A needle (0.3 \times 8 mm, 30 G) attached to a 0.3-mL U100 insulin syringe (BD Micro-Fine+, Heidelberg, Germany) was carefully inserted into the knee joint space and gently flushed twice with 25 μl of sterile saline. A total of 50 μl of synovial fluid lavage was recovered by aspiration and transferred into a tube. The synovial fluid samples were centrifuged twice for 2 min at 2100 rpm. The supernatant was frozen in dry ice and stored at $-80~^{\circ} C$ until used for cytokine analysis. The pellet was re-suspended with 100 μl of 5 % fetal bovine serum (Gibco-Thermo Fisher Scientific, Germany) in PBS and kept in ice until FACS analysis.

2.10. Flow cytometry – fluorescence activated cell sorting (FACS)

Blood and synovial fluid single-cell suspensions were centrifuged, and cell pellets were incubated for 15 min with 200 µg/mL mouse IgG (Jackson ImmunoResearch Laboratories) to block Fc γ -receptors. After washing with PBS supplemented with 5 % FCS (Sigma-Aldrich), cells were stained with fluorochrome-coupled antibodies for 20 min on ice and protected from light. Cells were washed and incubated with 100 nM SytoxBlue (LIFE technologies) for dead cell exclusion. Absolute cell numbers were quantified by addition of a defined number of 123 count eBeads (LIFE technologies) to the samples before analysis with a BD LSRFortessaTM (Becton Dickinson). Data were analyzed using FlowJo software (Treestar). The gating strategy is represented in Supplemental Fig. 1.

Antibodies used were: CD45-BV786 1:400 (A20; BioLegend), CD19-APC 1:400 (1D3; BD Biosciences), MHCII-A700 1:100 (M5/114.15.2; Invitrogen), CD11b-BV421 1:800 (M1/70; BioLegend), Ly6G-PerCP-Cy5.5 1:100 (1A8; BioLegend), Siglec-F-PE 1:100 (E50-2440; BD Biosciences), NK1.1-BV711 1:100 (PK136; BioLegend), Ly6C-APC-FIRE750 1:200 (HK1.4; BioLegend), and CD3-FITC 1:200 (17A2; BioLegend).

2.11. Cytokine bead assay

Blood plasma and synovial fluid cytokines were measured with the bead-based multiplex assays LEGENDplex $^{\rm TM}$ Mouse Inflammation or Th

Cytokine Panels (both BioLegend), according to the manufacturer's instructions.

2.12. Tissue preparation for histology

Mice were transcardially perfused with PBS (pH 7.4) followed by 4 % paraformaldehyde (PFA) solution at day 12 post-RSDS and day 35 post-KC. The knee joints (day 35 post-KC) and the brains (both time points) were collected and post-fixed in the same fixative overnight at 4 $^{\circ}\text{C}$. Samples were then stored in 0.5 % PFA at 4 $^{\circ}\text{C}$ until processing.

2.13. Knee histology

Knee joints were decalcified in 0.5 M ethylenediaminetetraacetic acid (EDTA, pH 7.4) on a shaker at 4 $^{\circ}$ C for ten days, changing the solution every third day. Decalcified samples were cryoprotected in 30 % sucrose in PBS for at least four days at 4 $^{\circ}$ C. After embedding in Tissue-Tek OCT cutting medium (Leica Biosystem), 16 μ m serial sections were cryo-cut in the coronal plane and thaw-mounted onto gelatin-coated slides for subsequent staining. Sections were stained for cartilage alterations (Safranin-O/ Fast Green protocol, see below) and synovium inflammation (Hematoxylin- Eosin staining, see below), imaged with a 4x objective using a Nikon microscope equipped with a DS-Fi3 camera (Y-TV55, Nikon Instruments, Düsseldorf, Germany) and scored as previously described (Glasson et al., 2010; Lewis et al., 2011; Schmitz et al., 2010).

2.13.1. Safranin-O/ Fast green staining

This staining allows identification of different joint compartments and detects cartilage alterations (Schmitz et al., 2010). Briefly, the procedure consists of consecutive baths in (1) Mayer Hematoxylin solution (Carl Roth, Karlsruhe, Germany), 8 min; (2) running tap water, 5 min; (3) Fast Green (Sigma, Steinheim, Germany) 0.05 % solution, 5 min; (4) 1 % acetic acid solution, 15 s; (5) Safranin-O (Sigma) 0.2 % solution, 5 min; (6) 100 % ethanol, 5 min; (7) 2x 100 % ethanol, 2 min; (8) xylene, 2 min. This results in the coloration of cartilage matrix in orange to red, the underlying bone in green, the nuclei in black, and the cytoplasm in grey-green. After drying, slides were cover slipped with Eukitt (O. Kindler, Freiburg, Germany). Bright-field images were obtained with a 4x objective using a Nikon microscope with a DS-Fi3 camera (Nikon Instruments, Amsterdam, The Netherlands). At least three sections per knee joint per mouse were examined and scored for cartilage degeneration, according to the Osteoarthritis Research Society International (OARSI) association (Glasson et al., 2010). This semiquantitative scoring system ranges from 0 to 6 as follows: 0, normal; 0.5, loss of Safranin-O without structural changes; 1, small fibrillations without loss of cartilage; 2, vertical clefts down to the layer immediately below the superficial layer and some loss of surface lamina; 3, vertical clefts/erosion to the calcified cartilage extending to < 25 % of the articular surface; 4, vertical clefts/erosion to the calcified cartilage extending to 25-50 % of the articular surface; 5, vertical clefts/erosion to the calcified cartilage extending to 50-75 % of the articular surface; 6, vertical clefts/erosion to the calcified cartilage extending > 75 % of the articular surface. All four joint quadrants (medial tibia, medial femur, lateral tibia, lateral femur) were analyzed, and the severity of cartilage changes was expressed as the summed score of the four quadrants per section and averaged between the different sections analyzed per mouse.

2.13.2. Hematoxylin- Eosin staining

This staining was used to detect the changes in synovial lining thickness and cellular density in the synovial stroma as a measure of synovial inflammation (Lewis et al., 2011; Schmitz et al., 2010). The protocol consisted of consecutive baths in (1) Mayer Hematoxylin solution (Carl Roth), 8 min; (2) running tap water, 5 min; (3) 95 % ethanol solution, 10 dips; (4) Eosin Y (Sigma) 0.25 % solution, 1 min; (5) 3x 100 % ethanol, 5 min; (6) xylene, 2 min. This results in the coloration of

cartilage matrix in pink, bone and fibrotic tissue in pink to red, nuclei in blue, and cytoplasm in pink to red. After drying, slides were cover slipped with Eukitt (O. Kindler, Freiburg, Germany). Bright-field images were obtained with a 4x objective using a Nikon microscope with a DS-Fi3 camera (Nikon Instruments, Amsterdam, The Netherlands). At least three sections per knee joint per mouse were examined and scored for synovitis, as previously reported (11). The score was obtained by evaluating the enlargement of the synovial lining cell layer (0 points, 1–2 cells thickness; 1 point, 2-4 cells thickness; 2 points, 4-9 cells thickness; 3 points, >10 cells thickness) and density of synovium stromal cells (0 points, normal cellularity; 1 point, cellularity slightly increased; 2 points, cellularity moderately increased; 3 points, cellularity greatly increased, pannus formation and rheumatoid-like granuloma might occur). The synovial insertion of the lateral femur, medial femur, lateral tibia, and medial tibia were evaluated, and the severity of synovial inflammation was expressed as the summed score of the four quadrants per section and averaged between the different sections analyzed per mouse.

2.13.3. Immunohistochemistry for macrophages and neutrophils

Joint sections were also used for immunohistochemistry to identify macrophages (F4/80, clone MB8, 123102, BioLegend, San Diego, USA) and neutrophils (Ly6G, clone 1A8, 127602, BioLegend). Briefly, sections were pretreated with antigen retrieval solution (2.94 % Tri-sodium citrate, AppliChem, Darmstadt, Germany, in distilled H2O, pH 6) for 20 min at 83 °C. Endogenous peroxidase was quenched with 1 % H₂O₂ in 1x PBS/ methanol (1:1) for 15 min. Sections were first incubated with 7 % normal serum in 0.2 % triton (Carl Roth, Karlsruhe, Germany) in PBS (PBST) for 30 min at room temperature to block unspecific binding and then with rat anti-mouse monoclonal antibodies (F4/80 or Ly6G) at 1:100 dilutions, overnight at 4 $^{\circ}\text{C}.$ Negative controls received blocking serum instead of the primary antibody. Then, following 3x 10 min washes with PBS, a rabbit anti-rat detection kit was used (Vectastin Elite ABC kit, Vector Laboratories, Burlingame, CA, USA), followed by 3,30-Diaminobenzidine (DAB) substrate (Vector Laboratories) for chromogenic detection and hematoxylin counter stain, as per manufacturer instructions. Digital images of the stained sections were obtained with a 10x objective using a Nikon microscope. Positive F4/80 or Ly6G cells were manually counted with ImageJ/Fiji software (National Institutes of Health, USA) and reported as the percentage of cells over the total cells in the area of interest.

2.14. Immunohistochemistry on brain sections

Brain coronal sections (50 µm) were cut with a vibratome (Leica VT1000S, Germany). Free-floating sections selected between Bregma + 1.98 mm and + 1.10 mm, spanning the rostral anterior cingulate cortex (rACC), prelimbic, (PrL), and infralimbic (IL) areas (12), were incubated in antigen retrieval solution (2.94 % Tri-sodium citrate in distilled H20, pH 6) for 20 min at 83 °C. After cooling to room temperature, the sections were incubated in 50 mM glycine (AppliChem) in PBS followed by PBST for ten minutes each, then blocked with 10 % normal horse serum (NHS) in PBS for 45 min. The sections were successively incubated with the primary antibody diluted in blocking solution overnight at 4 °C. The following primary antibodies were used: anti-Iba1 (rabbit, 1:500; 019-19741, Wako, Neuss, Germany) as a marker for microglia; anti-CD45 (rat, 1:200; MCA1388, Bio-Rad, Feldkirchen, Germany) as a marker for monocytes infiltrating the brain; anti- Δ FosB (rabbit, 1:2000; D3S8R, Cell Signaling, Leiden, The Netherlands) as a marker of sustained neuronal activation.

The sections were washed twice in 10 % horse serum in PBS for 10 min and incubated with the secondary antibody (1:700 dilution) in washing solution for one h at room temperature. Donkey anti-rabbit Alexa 488 (A-21206) was used for the Iba-1 staining, donkey anti-rat Alexa-594 (A-21209) was used for the CD45 staining, and donkey anti-rabbit Alexa-594 (A-21207) was used for the Δ FosB staining (all

from Thermo Fischer Scientific, Darmstadt, Germany). The sections were rewashed and incubated in Hoechst (#H3670, 1:10 000 in PBS, Thermo Fischer Scientific) for 10 min. Tissues were washed three times in PBS for 10 min and incubated for 10 min in 10 mM TRIS-HCl before mounting with Mowiol (Sigma-Aldrich).

Stained sections for Iba-1 and CD45 were imaged by using a confocal laser-scanning microscope (Leica TCS SP8 AOBS, Wetzlar, Germany) with a 20x objective (Leica, 20X/0.75, HC PL APO). Images were acquired in the sequential line scan mode with a 1024x1024 resolution over a 25 μm depth (Z-step: 2.5 μm , 10 steps) in the target regions defined by the Paxinos and Franklin atlas (Franklin and Paxinos, 2013). Sections stained for $\Delta FosB$ were imaged with an epifluorescence microscope equipped with a DS-Qi2 camera (10 \times objective; Nikon). The mean signal intensity of Iba-1 immunoreactivity, number of CD45 positive cells per mm^2 , and count of $\Delta FosB$ positive cells per mm^2 was measured using ImageJ/Fiji software (National Institutes of Health).

At least three brain sections per each rostral anterior cingulate cortex (rACC) prelimbic, (PrL), and infralimbic (IL) areas per mouse were stained, imaged, and analyzed with ImageJ/Fiji, using the same settings for all the sections and mouse groups.

For Iba-1, the mean signal intensity was measured using a region of interest (ROI; 270.44 μm x 270.44 μm) to measure the intensity on three different locations of each brain area per section. The resultant values were averaged for the respective brain areas of each mouse.

For CD45 staining, the positive cells were manually counted using the ImageJ/Fiji cell counter plug-in on the whole rACC, PrL, and IL areas of each section because the presence of these cells in the brain is very sparse.

For $\Delta FosB$, positive neurons on the whole rACC area were quantified using the automatic "particle analysis" counting option with a fixed configuration that only detected pixels that matched a certain range of size and circularity. Before running the particle analysis counter, a fixed threshold interval was set to distinguish the $\Delta FosB$ positive neurons from the background and convert the image in binary. Additionally, the "watershed separation" was applied on the binary images to separate $\Delta FosB$ positive neurons, which are too close and overlap, for more accurate counting.

2.15. Statistical analyses

Statistical analyses were performed with Graph Pad Prism (version 9.0). One and two-way random measures ANOVA, and two-way repeated measures ANOVA followed by Tukey's post-hoc multiple comparisons were used when a main effect or significant interaction between two main factors was indicated. The differences were considered statistically significant when $P<0.05.\ F$ and P values from all experimental groups shown in the main figures are listed in Supplemental Table 1.

3. Results

3.1. Repeated social defeat stress (RSDS) drives resilience versus susceptibility with distinct phenotypes in male mice

Following ten days of RSDS, male mice were tested for SI performances to distinguish between resilient and susceptible populations according to their SI ratio (Golden et al., 2011) (Fig. 1A). Susceptible mice (SI ratio < 1) avoided interaction with the target (aggressor) and spent significantly more time in the corners of the SI arena (Fig. 1B). In contrast, resilient mice (SI ratio \geq 1) interacted more with the target and spent similar time in the corners as control mice which were never exposed to RSDS (Fig. 1B). As an index of stress hormones at the end of RSDS, fecal corticosterone metabolite (FCM) levels were measured (Fig. 1A) and found to be similarly increased in both resilient and susceptible groups compared to controls (Fig. 1C).

Male mice were then characterized for their emotional-like behavior

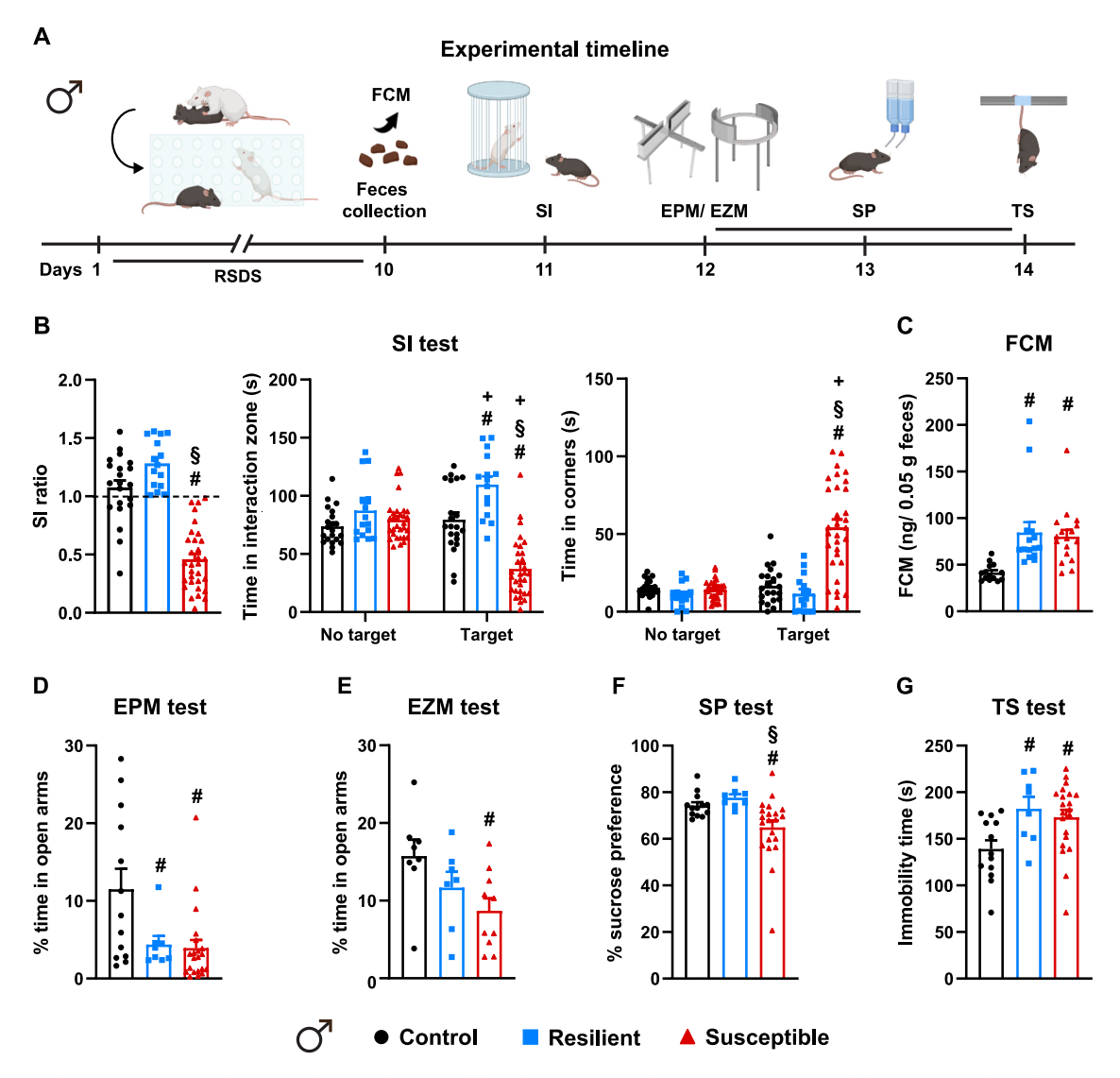


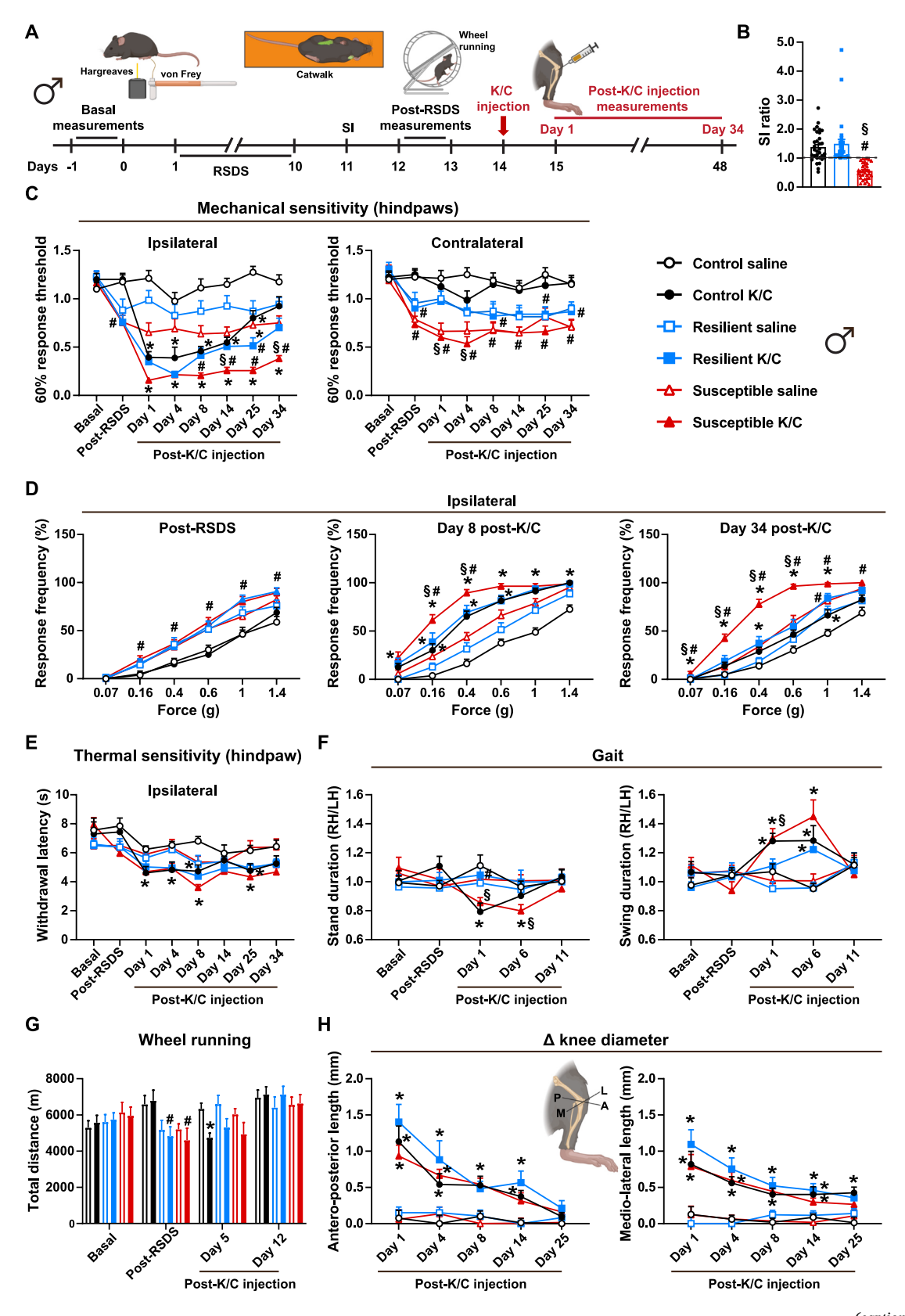
Fig. 1. Distinct phenotypes in RSDS-driven resilient and susceptible male mice. (A) Schematic representation of the experimental timeline. RSDS was applied for ten days, followed by the analysis of FCMs. Behavior was assessed on the following four subsequent days for social avoidance with the SI test, anxiety-like behavior with EPM or EZM, anhedonia-like behavior with SP, and depression-like behavior with TS test. (B) SI ratio (left panel), time in the interaction zone (middle panel), and time in corners (right panel) during the absence (no target) or the presence (target) of the aggressor mouse in the SI test (n = 15-31/group). (C) FCM levels were measured after RSDS (n = 14-17/group). (D) Percentage of time spent in the open arms of the EPM (n = 8-21/group). (E) Percentage of time spent in the open arms of the EZM (n = 7-10/group). (F) Percentage of sucrose intake in the SP test (n = 8-21/group). (G) Immobility time in the TS test (n = 8-21/group). Data are expressed as mean \pm SEM with individual data points representing individual mice. P < 0.05 indicated by # compared to the control group, \S compared to the resilient group, \pm compared to "No target" time-point within a group; one-way ANOVA (B, C left panel, D, E, F, G) or two-way repeated measures ANOVA with Tukey-post-hoc-test (C, middle and right panel). See Supplemental Table 1 for further statistical information. ANOVA, analysis of variance; EPM, elevated plus maze; EZM, elevated zero maze; FCM, fecal corticosterone metabolites; RSDS, repetitive social defeat stress; SI, social interaction; SP, sucrose preference; TS, tail suspension.

(Fig. 1A). In the EPM test, both resilient and susceptible mice showed increased anxiety-like behavior, as indicated by a significant reduction of the % time spent in open arms as compared to controls (Fig. 1D). However, in EZM (different mouse cohort) we observed increased anxiety only in susceptible mice, spending significantly less % time in open quadrants compared to resilient and controls (Fig. 1E). Along the same line, susceptible mice also displayed increased anhedonia, indicated by a significant reduction of sucrose preference compared to resilient and control mice (Fig. 1F). In contrast, both resilient and susceptible mice showed increased behavioral despair, indicated by significantly increased immobility time in the TS test compared to controls (Fig. 1G).

These data indicated that resilient and susceptible male mice displayed increased FCM levels and despair behavior, but only susceptible mice developed social avoidance, anhedonia and pronounced anxiety. 3.2. Knee arthritis-associated pain behavior was exacerbated and prolonged in susceptible male mice

Psychosocial stress represents a risk factor for the aggravation and chronicity of inflammatory diseases, including arthritis (Evers et al., 2014; Johnson et al., 2019; Musich et al., 2019; Sawicki et al., 2020). In male mice, we investigated the influence of RSDS on direct and movement-related pain measures and joint swelling in a model of knee arthritis induced by intra-articular K/C injection into the right knee (Fig. 2A). Mice were divided into resilient or susceptible groups according to their SI ratio (Fig. 2B).

RSDS by itself induced mechanical hypersensitivity in both resilient and susceptible mice, indicated by a significant reduction of the post-RSDS 60 % response threshold at both hindpaws versus controls and



(caption on next page)

Fig. 2. Worsened and prolonged pain behavior associated with knee arthritis in susceptible male mice. (A) Scheme of the experimental protocol; RSDS combined with the K/C model. After basal pain-related behavior measurements (von Frey, Hargreaves, Catwalk, wheel running), RSDS was applied for ten days, followed by the SI test, pain-related behavior evaluation, arthritis induction with K/C injection into the right knee articular space, and further pain behavior analysis at different post-injection time points. (B) SI ratio categorizing susceptible and resilient mice in the SI test (n = 29-34/group). (C) Mechanical sensitivity towards graded von Frey filaments (60 % response threshold) at ipsilateral and contralateral hindpaws (n = 14-17/group). (D) Mechanical sensitivity at the ipsilateral hindpaw, shown as the response frequency towards individual graded von Frey filaments at post-SDS, day eight and day 34 post-K/C injection (n = 14-17/group). (E) Thermal sensitivity to radiant heat, measured with the plantar test apparatus as the withdrawal latency of the ipsilateral hindpaw (n = 5-9/group). (F) Gait analysis showing the RH/LH ratio for stand duration (left panel) and swing duration (right panel) (n = 11-12/group). (G) Voluntary wheel running activity measured as total run distance (n = 11-12/group). (H) Δ knee diameter (difference between the right and left knee diameter) along the antero-posterior and medio-lateral axes (n = 11-12/group). Data are expressed as mean \pm SEM with individual data points representing individual mice. P < 0.05 indicated by * compared to the respective saline group, # compared to the control group, § compared to the resilient group; one-way ANOVA (B) or two-way repeated measures ANOVA (C-H) with Tukey-post-hoctest. In (C-H), statistically significant post-hoc differences are only indicated for K/C groups to simplify the readability of the data. See Supplemental Table 1 for further statistical information. ANOVA, analysis of variance; K/C, kaolin/carrageenan; LH, le

basal measurement (Fig. 2C; see Supplemental Table 1 for detailed statistical analysis of all result parts) and increased response frequency to vF filaments at this time-point (Fig. 2D, left panel). The mechanical hypersensitivity persisted throughout the observation period (reduced 60 % response threshold in saline stress groups) and was more pronounced in susceptible compared to resilient mice (Fig. 2C).

Within one day after K/C injection, mechanical hypersensitivity developed explicitly at the ipsilateral hindpaw of control mice and stress groups compared to the respective saline groups and the post-RSDS (preinjection) time-point (Fig. 2C). Contralateral paw sensitivity was not further affected (Fig. 2C). The K/C-induced ipsilateral hypersensitivity was similar in control and resilient mice at all post-injection time-points (except day 25 post-K/C) and returned to pre-injection values at day 34 (Fig. 2C). In contrast, susceptible mice showed exacerbated ipsilateral mechanical hypersensitivity, indicated by a significantly lower 60 % response threshold compared to controls (from day 8 to 34 post-K/C) and resilient mice (day 14 and 34 post-K/C) (Fig. 2C) and increased response frequency to vF filaments compared to both groups (Fig. 2D, day 8). Interestingly, the K/C-induced mechanical hypersensitivity in susceptible mice did not recover until day 34 post-K/C, as seen in control and resilient mice (Fig. 2C; 2D, day 34).

Thermal sensitivity was not affected by RSDS. The withdrawal latencies of all mouse groups were comparable between baseline and post-RSDS time points (Fig. 2E). K/C injection increased heat sensitivity at the ipsilateral hindpaw of control mice versus the respective saline group at almost all post-injection time-points, except for days 14 and 34, and in susceptible mice at days 8 and 25, but not in resilient mice (Fig. 2E). No significant differences were observed between K/C groups.

An antalgic gait often accompanies arthritis (Ängeby Möller et al., 2020). Therefore, we evaluated the walking patterns on the Catwalk. RSDS did not affect the gait. All mouse groups showed similar hindpaw ratios (right hindpaw over left hindpaw, RH/LH) for stand (contact time with the floor) and swing (lifting time) at the post-RSDS time-point (Fig. 2F). K/C-injection in control mice transiently reduced the ratio for stand duration on day 1 and increased the swing duration at days 1 and 6 post-K/C (Fig. 2F). Resilient K/C mice showed only a delayed increase of swing duration ratio at day 6 post-K/C (Fig. 2F). In contrast, susceptible K/C mice displayed prolonged gait alterations: stand and swing duration ratios were significantly different at day 1 and 6 post-K/C and returned to pre-injection levels only at day 11 (Fig. 2F).

RSDS by itself affected wheel-running activity. Resilient and susceptible groups run less than controls at the post-SDS time-point (Fig. 2G). K/C injection transiently impaired the running activity in control mice at day 5 post-K/C. Resilient and susceptible mice did not show a further reduction in running distance following K/C injection (day 5) and normalized their running profile as control K/C mice at day 12 post-K/C (Fig. 2G).

To assess arthritis-associated joint swelling, we measured the knee diameter along the antero-posterior and medio-lateral joint axes. K/C injection induced similar joint swelling (displayed as the difference between right and left joint diameter) in all groups from day 1, which was completely recovered by day 25 post-injection, except for a higher medio-lateral length in control K/C versus saline (Fig. 2H).

Thus, RSDS promoted a long-lasting increase in mechanical sensitivity and a short-lasting decrease in wheel running activity without alteration of thermal sensitivity or gait in male mice. K/C injection in control male mice transiently induced joint swelling, mechanical and thermal hypersensitivity, gait, and running activity impairment. Interestingly, susceptible K/C male mice displayed exacerbated and longer-lasting mechanical hypersensitivity, as well as prolonged gait alterations compared to control and resilient K/C male mice. However, the duration and levels of joint swelling were comparable between all groups.

3.3. K/C-induced Mechanical hypersensitivity was prolonged but not exacerbated in susceptible female mice

Next, we repeated the same experimental procedures in female mice to assess potential sex differences and performed the most relevant tests associated with behavioral alterations in this model (Fig. 3A).

Female mice were separated into resilient and susceptible groups according to their SI ratio (Fig. 3B). We did not observe differences in FCM levels between groups (Fig. 3C). However, both resilient and susceptible female mice showed increased anxiety-like behavior compared to controls in the EZM test (Fig. 3D). Still, only susceptible female mice displayed increased anhedonia compared to control mice in the SP test (Fig. 3E).

Following RSDS, resilient and susceptible female mice showed similarly increased mechanical sensitivity, as the post-RSDS 60 % response threshold at both hindpaws of resilient and susceptible groups were reduced versus controls and basal measurement (Fig. 3F). The mechanical hypersensitivity was still present at day 1, but it did not persist throughout the observation period, since at the subsequent time-points susceptible and resilient mice (saline groups) had similar 60 % thresholds than controls at both hindpaws, except for susceptible saline (ipsilateral paw) at day 14 (Fig. 3F).

Within one day after K/C injection, mechanical hypersensitivity developed at the ipsilateral hindpaw of control mice and further in stress groups compared to the respective saline groups (Fig. 3F). Contralateral paw sensitivity was not further affected (Fig. 3F). The K/C-induced ipsilateral hypersensitivity was similar in control and stress mice at all post-injection time-points (Fig. 3F). However, in resilient K/C group, it was only significant at post-K/C days 1 and 14 (Fig. 3F). Mechanical hypersensitivity recovered completely at day 34 in control and resilient mice, but not in susceptible mice, as indicated by the lower 60 % response threshold (Fig. 3F, left panel) and the higher response frequency to 0.16–1 g filaments (Fig. 3F, right panel) of the susceptible K/C mice versus control and resilient K/C mice at day 34.

These results indicated that, similarly to male mice, the K/C-induced mechanical hypersensitivity was prolonged in susceptible females, although its severity was not affected.

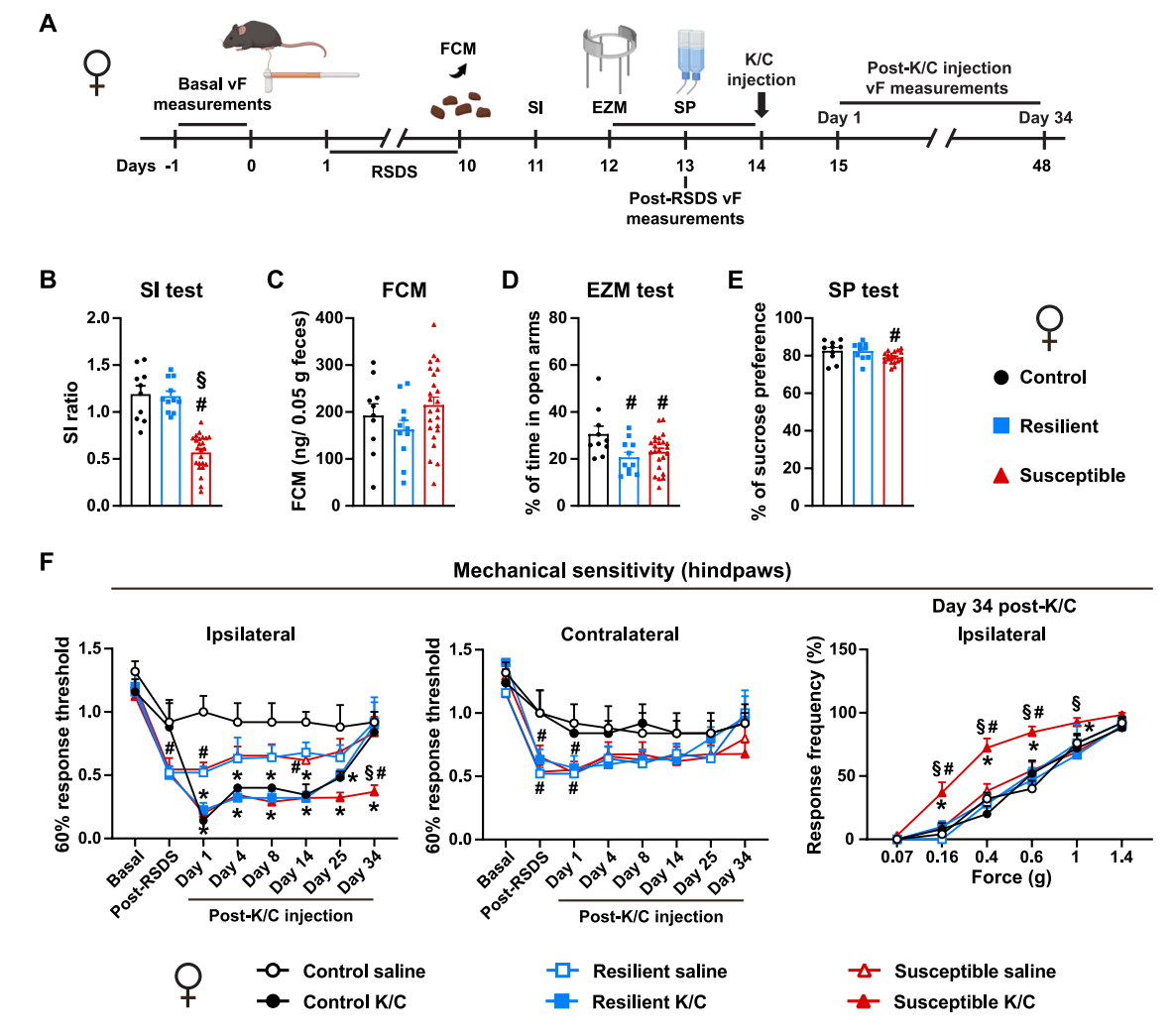


Fig. 3. Prolonged but not exacerbated K/C-induced mechanical hypersensitivity in susceptible female mice. (A) Scheme of the experimental protocol. After basal von Frey measurements, RSDS was applied for ten days, followed by the analysis of FCM. Behavior was assessed on the following four subsequent days for social avoidance with the SI test, anxiety-like behavior with EZM, anhedonia-like behavior with SP and post-RSDS mechanical sensitivity with von Frey. Arthritis was subsequently induced by knee K/C injection, and further mechanical sensitivity analysis was performed with von Frey at different post-injection time points. (B) SI ratio categorizing susceptible and resilient female mice in the SI test (n = 10-24/group). (C) FCM levels (n = 10-24/group). (D) Percentage of time spent in the open arms of the EZM (n = 10-24/group). (E) Percentage of sucrose intake in the SP test (n = 10-24/group). (F) Mechanical sensitivity towards graded von Frey filaments shown as 60 % response threshold at ipsilateral and contralateral hindpaws (left and middle panel, respectively; n = 5-13/group) and response frequency of the ipsilateral hindpaw towards individual von Frey filaments at day 34 post-K/C injection (right panel; n = 5-13/group). Data are expressed as mean \pm SEM with individual data points representing individual mice. P < 0.05 indicated by * compared to the respective saline group, # compared to the control group, § compared to the resilient group; one-way ANOVA (B-E) or two-way repeated measures ANOVA (F) with Tukey-post-hoc-test. See Supplemental Table 1 for further statistical information. ANOVA, analysis of variance; EZM, elevated zero maze; FCM, fecal corticosterone metabolites; K/C, kaolin/carrageenan; RSDS, repetitive social defeat stress; SI, social interaction; SP, sucrose preference, vF, von Frey.

3.4. Circulating leukocyte and cytokine levels were differentially regulated following RSDS and joint inflammation in control, resilient and susceptible male mice

Bidirectional interactions between the peripheral immune system and CNS are recognized to play a crucial role in stress-related disorders and chronic pain (Ader et al., 1995; Cathomas et al., 2019; Geraghty et al., 2021; Hodes et al., 2014; Niraula et al., 2018; Raison et al., 2006; Sawicki et al., 2020; Wohleb et al., 2015). To analyze the effect of RSDS on the peripheral immune system and its potential priming effect on arthritis, we evaluated blood immune cell and cytokine profiles at different time points in male mice (Fig. 4A).

At the end of the stress protocol (day 12 post-RSDS), both resilient and susceptible mice showed significantly decreased B cells, a trend for reduced T cells, and increased neutrophil and Ly6C^{high} monocyte frequencies compared to control mice (Fig. 4B). Frequencies of NK cells,

eosinophils and Ly6C^{low} monocytes were unaltered (Fig. 4B). Interestingly, these changes were transient in resilient mice (saline group), as the frequency of these cells returned to control levels at the subsequent time-points (Fig. 4C, D), except for neutrophils, which were significantly lower at day 35 compared to control saline mice (Fig. 4D). In contrast, in susceptible mice, the frequencies of B and T lymphocytes remained significantly lower and neutrophils significantly higher on day 5 (Fig. 4C), and B cell frequency lower than resilient saline mice at day 35 (Fig. 4D), with no further changes of other cell subtypes at these time-points (Fig. 4C, D).

Following arthritis induction, in control K/C mice, we observed only a significant decrease of neutrophil frequency at day 35 post-injection compared to control saline (Fig. 4D). Resilient K/C mice displayed decreased B and T cells and increased neutrophil frequencies at day 5 post-injection (Fig. 4C) and increased Ly6C^{high} monocyte frequency at day 35 post-injection (Fig. 4D) compared to resilient saline mice. In

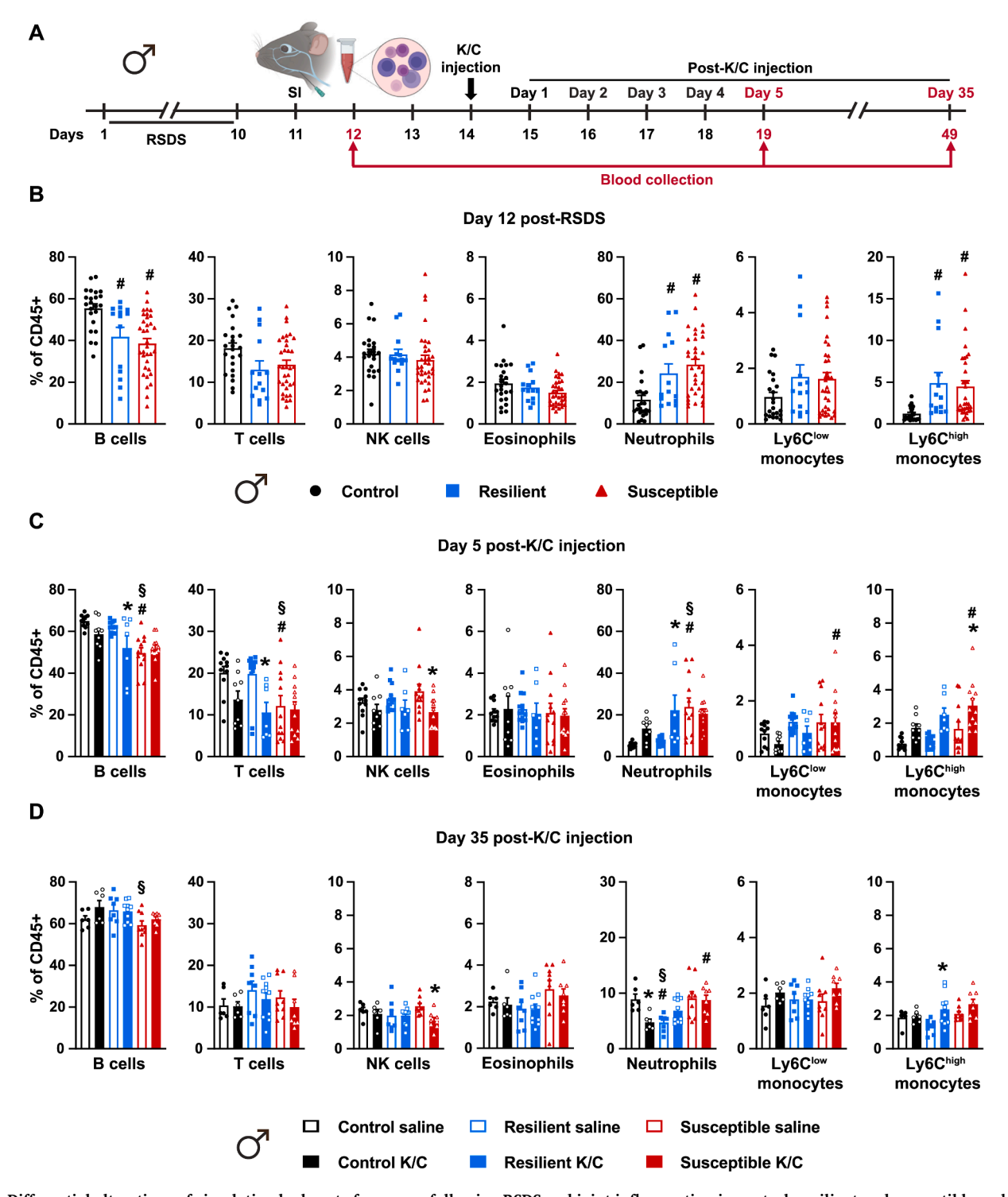


Fig. 4. Differential alterations of circulating leukocyte frequency following RSDS and joint inflammation in control, resilient and susceptible male mice. (A) Schematic representation of the experimental timeline for blood collection and FACS analysis at day 12 post-RSDS, day 5 and day 35 post-K/C injection time-points (day 19 and day 49 post-RSDS, respectively). Relative frequencies of B cells, T cells, NK cells, eosinophils, neutrophils, Ly6C^{low} and Ly6C^{high} monocytes, calculated as the percentage of total CD45 + cells in peripheral blood at (B) day 12 post-RSDS (n = 14–34/group), (C) day five post-K/C (n = 7–14/group) and (D) day 35 post-K/C (n = 6–10/group). Data are expressed as mean \pm SEM with individual data points representing individual mouse samples. P < 0.05 indicated by * compared to the respective saline group, # compared to the control group, § compared to the resilient or susceptible group; one-way ANOVA (B) or two-way ANOVA (C-D) with Tukey-post-hoc-test. See Supplemental Table 1 for further statistical information. ANOVA, analysis of variance; FACS, fluorescence-activated cell sorting; K/C, kaolin/carrageenan; NK, natural killer cells; RSDS, repetitive social defeat stress; SI, social interaction.

contrast, susceptible K/C mice showed significantly lower NK cell frequency compared to susceptible saline at days 5 (Fig. 4C) and 35 post-KC (Fig. 4D), higher Ly6C^{high} monocyte frequency compared to susceptible saline and control K/C at day 5 post-injection (Fig. 4C) and higher

neutrophil frequency than control K/C at day 35 post-injection (Fig. 4D). Summarizing, RSDS induced similar changes in specific blood leukocyte subtypes in resilient and susceptible male mice. These changes were transient but lasted longer in susceptible than in resilient male

mice and, thus, may have contributed to the aggravated pain-related behavior in these mice. Joint inflammation further regulated blood cell frequency, with NK cells, neutrophils, and Ly6Chigh monocytes being the most differentially modulated between control and RSDS groups.

Additionally, cytokine levels were measured in plasma (Supplemental Table 2). At day 12 post-RSDS, interleukin (IL)-6 and IL-17A were significantly increased in both resilient and susceptible mice, whereas IL-1 α , IL-10, IL-12, IL-23 and GM-CSF were increased only in resilient mice, and IL-27 decreased only in susceptible mice (Supplemental Table 2). At day 5, IL-10, IL-17A and IL-22 levels remained higher in resilient saline mice, while none of the cytokines was altered in susceptible saline mice (Supplemental Table 2). Likewise, at day 35, resilient saline mice showed higher IL-10 and IL-17F levels (Supplemental Table 2). In contrast, susceptible saline mice displayed lower IL-12 and IL-27, and higher IL-17A levels (Supplemental Table 2).

K/C injection differentially regulated the circulating cytokines in control and RSDS groups. In control K/C mice, tumor necrosis factor (TNF)- α was the only cytokine significantly upregulated at day 5, whereas IL-12 was downregulated and IL-27 upregulated at day 35 (Supplemental Table 2). Interestingly, arthritis induction did not affect cytokine levels in resilient mice. Like the resilient saline group, resilient K/C showed higher IL-10 levels at day 35 post-injection (Supplemental Table 2). In contrast, susceptible K/C mice displayed not only higher TNF- α levels like controls K/C but also higher IL-6 levels at day 5, and higher IL-12 and IL-22, and lower IL-27 levels at day 35 post-K/C (Supplemental Table 2).

Overall, among the RSDS-regulated cytokines, IL-10 was consistently higher in resilient male mice throughout the observation period, suggesting a potential role of this anti-inflammatory cytokine (Molnar et al., 2021) in regulating pain behavior in these mice. Conversely, the proinflammatory IL-6 (Molnar et al., 2021) might contribute to the mechanical hypersensitivity in RSDS groups and exacerbated pain in susceptible male mice following arthritis induction at the early stage. IL-12 and IL-27 might be more involved at the late arthritis stage, as they were differentially regulated in control, resilient and susceptible male mice at the late time-point.

Furthermore, we measured FCM levels at days 7 and 33 post-K/C injection but did not observe significant changes between the groups (Supplemental Table 3). This indicated that the regulation of circulating immune cells and cytokines at the post-K/C stages was independent of corticosterone modulation.

3.5. The density of neutrophils and macrophages in the inflamed knee joint synovium was increased in male susceptible mice

We performed histological analysis of the right knee joints in male mice at the end of the experiments (day 35 post-K/C injection) to assess the grade of cartilage alterations and synovial inflammation promoted by K/C, as a potential source for the behavioral differences at the late arthritis stage.

However, we did not find any difference between the groups concerning cartilage alterations (Fig. 5A). Despite the recovery of all pain-related alterations in control and resilient mice at this late time-point (Fig. 2), all K/C groups similarly showed a higher inflammation score, globally reflected by increased thickness of the synovial lining layer and cellularity, compared to the respective saline groups (Fig. 5B).

Nevertheless, we further examined the synovium of male mice at day 35 post-K/C injection for the presence of neutrophils and macrophages, the cells involved in synovial inflammation, and associated with worsening osteoarthritis progression and pain (Hsueh et al., 2021).

The percentage of neutrophils (Ly6G positive cells) was comparable among all saline groups, but it was significantly increased in resilient and susceptible K/C (not in control K/C), being higher in susceptible K/C compared to control K/C (Fig. 5C). This indicated that RSDS did not affect the basal levels of neutrophils in the synovium in male mice. Still, it induced a higher density of these cells in the context of joint

inflammation.

The percentage of macrophages (F4/80 positive cells) was unexpectedly increased in the RSDS saline groups only in resilient mice. Following K/C injection, it was increased in control and susceptible K/C but not further regulated in resilient K/C group (Fig. 5D). Interestingly, it was significantly higher in susceptible K/C compared to control K/C mice (Fig. 5D).

The levels of immune cells and cytokines were also analyzed in the synovial fluid from knee joints of male mice at day 35 post-K/C injection to investigate whether local changes in immune parameters were associated with the observed differences in pain between groups (Fig. 5E and Supplemental Table 4).

RSDS did not induce major changes in synovial fluid leukocyte frequencies (Fig. 5E). However, in the RSDS saline groups only resilient mice showed a significantly higher frequency of NK cells (Fig. 5E). Except for a significant increase of Ly6C low frequency in resilient K/C, none of the cells was significantly altered by K/C injection in the other groups (Fig. 5E).

Analysis of synovial fluid cytokines revealed that IL-2, IL-12, IL-13, IL-17F, IL-22 and TNF α were differentially regulated in the synovial fluid of RSDS saline groups compared to the control saline group (Supplemental Table 4). Following K/C injection, the only cytokine affected in controls was IL-12, being significantly lower compared to saline mice (Supplemental Table 4). Similar lower IL-12 levels were also present in resilient K/C. In contrast, IL-12 levels were already low in susceptible mice independently from K/C injection (Supplemental Table 4). Moreover, resilient K/C mice showed significantly higher levels of IL-27, MCP-1 and GM-CSF, as well as lower IL-22, IL-17F, and TNF α levels versus resilient saline mice having significantly higher levels of these cytokines (Supplemental Table 4). Susceptible K/C mice only showed significantly lower IL-2, IL-22 and TNF α levels versus susceptible saline having higher levels of these cytokines (Supplemental Table 4).

3.6. Microglia expression and monocyte infiltration were increased in the rACC of susceptible male mice following joint inflammation

Following RSDS, peripheral monocytes infiltrate specific brain areas and interact with other immune mediators to regulate neuro-inflammation and promote RSDS-associated behavioral alterations (Calcia et al., 2016; Cathomas et al., 2019; McKim et al., 2018; Nie et al., 2018; Wohleb et al., 2015). Therefore, we next investigated brain neuroinflammation by assessing microglia expression and monocyte infiltration directly after RSDS exposure (day 12) and at the late time point (day 35) after K/C injection in male mice. We focused on the rACC, PrL and IL areas (Fig. 6A), which are associated with RSDS (McKim et al., 2018; Nie et al., 2018) and pain processing (Kummer et al., 2020; Serafini et al., 2020), also during arthritis (Abe et al., 2022).

RSDS induced an increase of microglia expression in these brain regions, as indicated by higher fluorescence intensity of the Iba-1 marker in resilient and susceptible male mice in the right and left hemispheres of rACC, PrL and IL regions at day 12 post-SDS (Fig. 6B). However, this RSDS-induced change was transient because at day 35 post-injection the fluorescence intensity was similar in all saline groups in these regions (Fig. 6C). Interestingly, K/C injection induced increased microglia expression at this time-point only in susceptible, but not in control and resilient male mice, in both right and left rACC, PrL and IL (Fig. 6C).

Moreover, RSDS induced infiltration of CD45-positive cells (Fig. 7A), a marker enriched on and used for visualization of monocytes/macrophages in the CNS (McKim et al., 2018; Nie et al., 2018; Sawicki et al., 2019; Torres-Platas et al., 2014; Zhang et al., 2014, 2012), only in the rACC of susceptible male mice, but not PrL and IL (Fig. 7B). This change was also transient. At day 35 post-injection, CD45-positive cell numbers were similar in all saline groups in the three regions analyzed (Fig. 7C). Notably, K/C injection increased CD45-positive cell number at this time-point only in susceptible male mice in both rACC sides, but not in PrL and IL (except for higher CD45-positive cell number in the right IL as

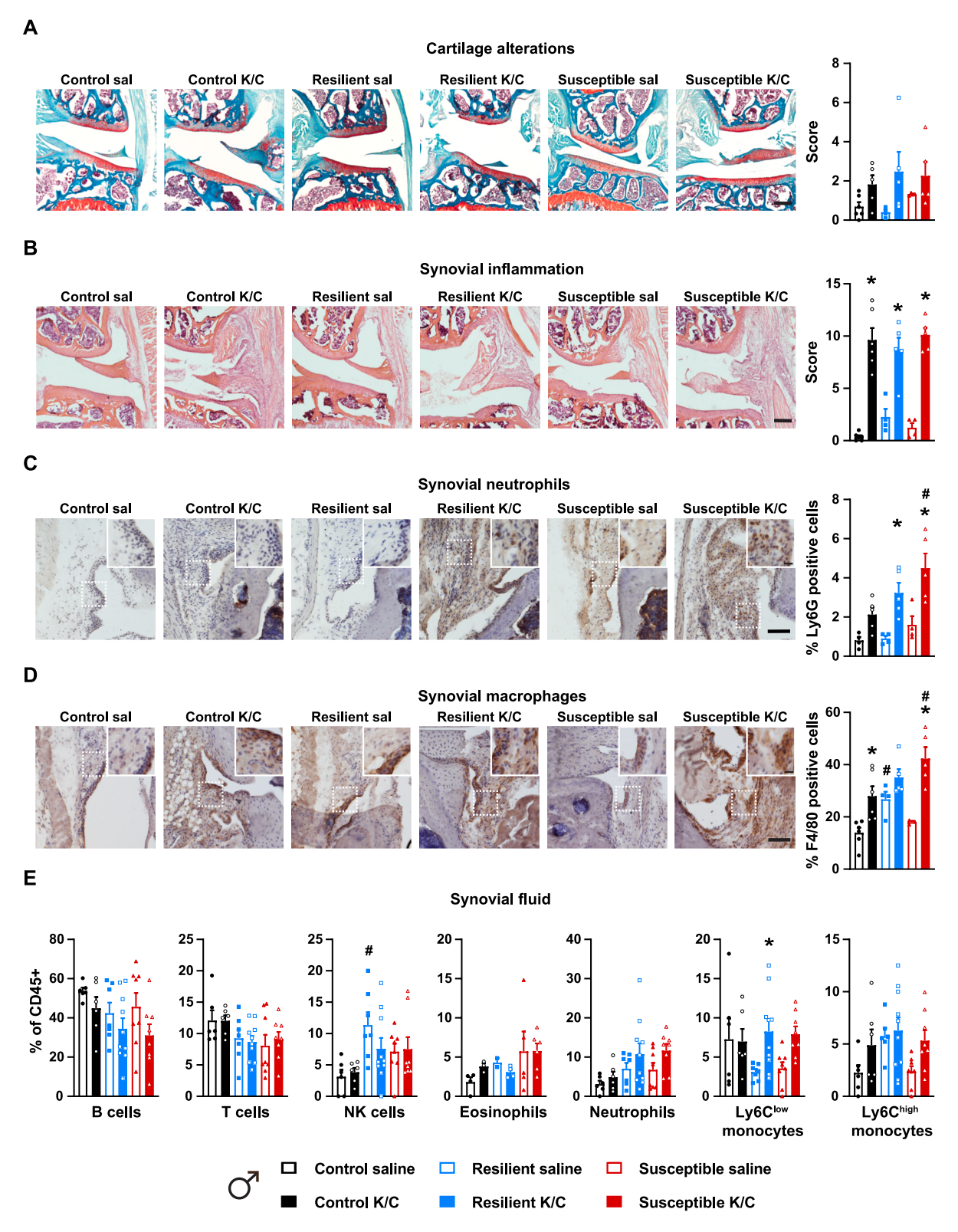


Fig. 5. Increased density of neutrophils and macrophages in the inflamed knee joint synovium of susceptible male mice. Representative images and quantification of right knee joint coronal sections at day 35 post-K/C stained with (A) Safranin-O-Fast green to grade cartilage alterations (n = 4-6/group), (B) Hematoxylin-Eosin to assess synovial inflammation (n = 4-6/group), (C) Ly6G marker to measure synovial neutrophil infiltration (n = 4-5/group) and (D) F4/80 marker to measure synovial macrophage infiltration (n = 3-6/group). (E) Relative frequencies of B cells, T cells, NK cells, eosinophils, neutrophils, Ly6C^{low} and Ly6C^{high} monocytes, calculated as the percentage of total CD45 + cells in the synovial fluid collected at the end of the experiments (day 35 post-K/C injection) (n = 6-10/group). Data are expressed as mean \pm SEM with individual data points representing individual mouse samples. P < 0.05 indicated by * compared to the respective saline group, # compared to the control group; two-way ANOVA. See Supplemental Table 1 for further statistical information. Scale bar: 200 μ m in (A) and (B), 100 μ m in (C) and (D) and 200 μ m in magnified images in (C) and (D). ANOVA, analysis of variance; K/C, kaolin/carrageenan; NK, natural killer cells; sal, saline.

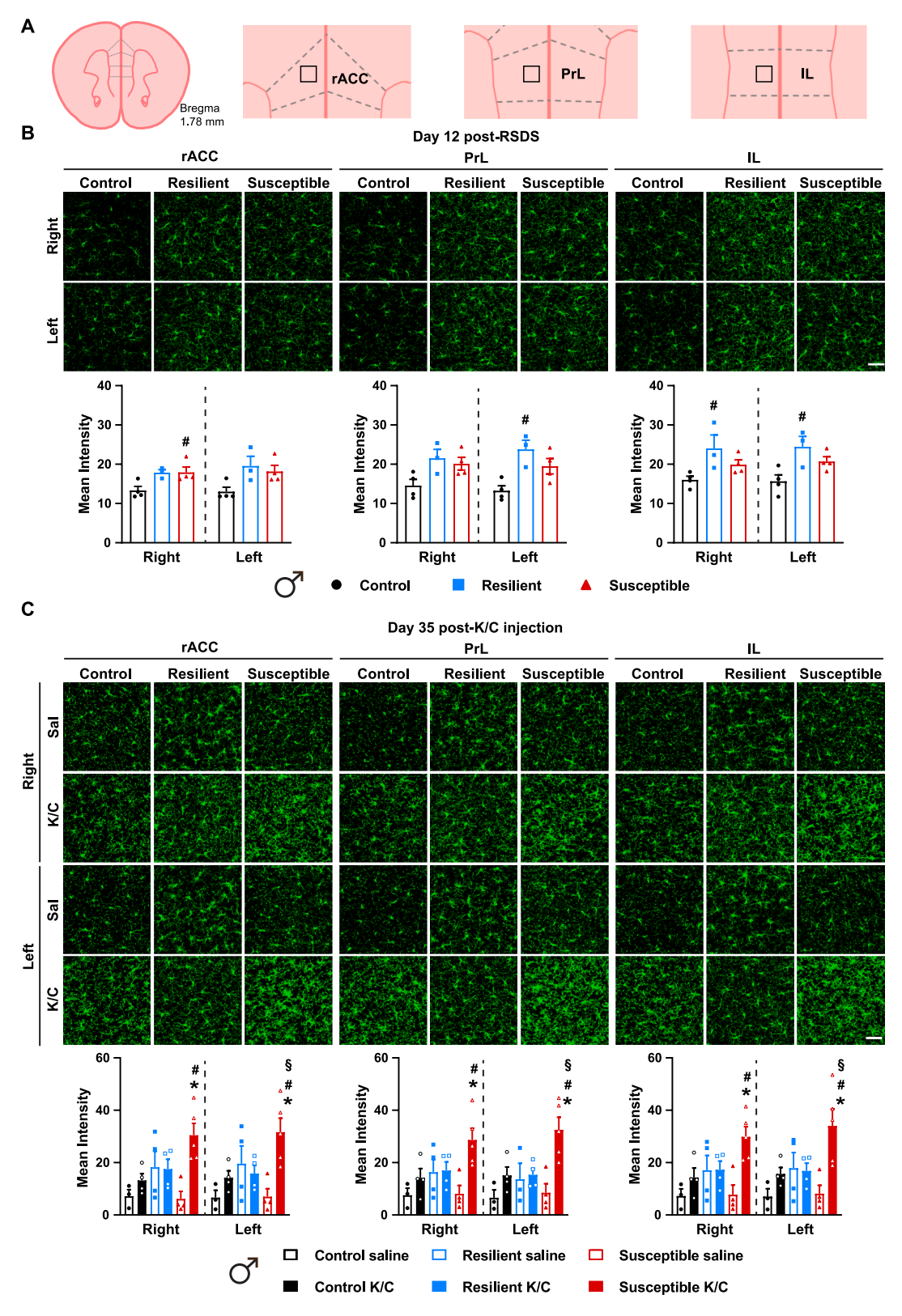


Fig. 6. Increased microglia expression in rACC, PrL and IL following joint inflammation in susceptible male mice. (A) Schematic illustration of one of the representative brain coronal sections used for Iba-1 immunostaining in rACC, PrL and IL areas. The black box drawn in each brain area depicts the ROI used to quantify the staining. (B-C) Representative images and quantification (mean intensity) of Iba-1 immunostaining in the right and left sides of rACC, PrL and IL at day 12 post-SDS (B, n = 3–4/group) and day 35 post-K/C injection (C, n = 3–5/group). Data are expressed as mean \pm SEM with individual data points representing individual mouse samples. P < 0.05 indicated by * compared to the respective saline group, # compared to the control group; § compared to the resilient group; one-way ANOVA (B) or two-way ANOVA (C) with Tukey-post-hoc-test. See Supplemental Table 1 for further statistical information. Scale bar: 50 μ m. ANOVA, analysis of variance; IL, infralimbic area; K/C, kaolin/carrageenan; PrL, prelimbic area; rACC, rostral anterior cingulate cortex; ROI, region of interest; sal, saline.

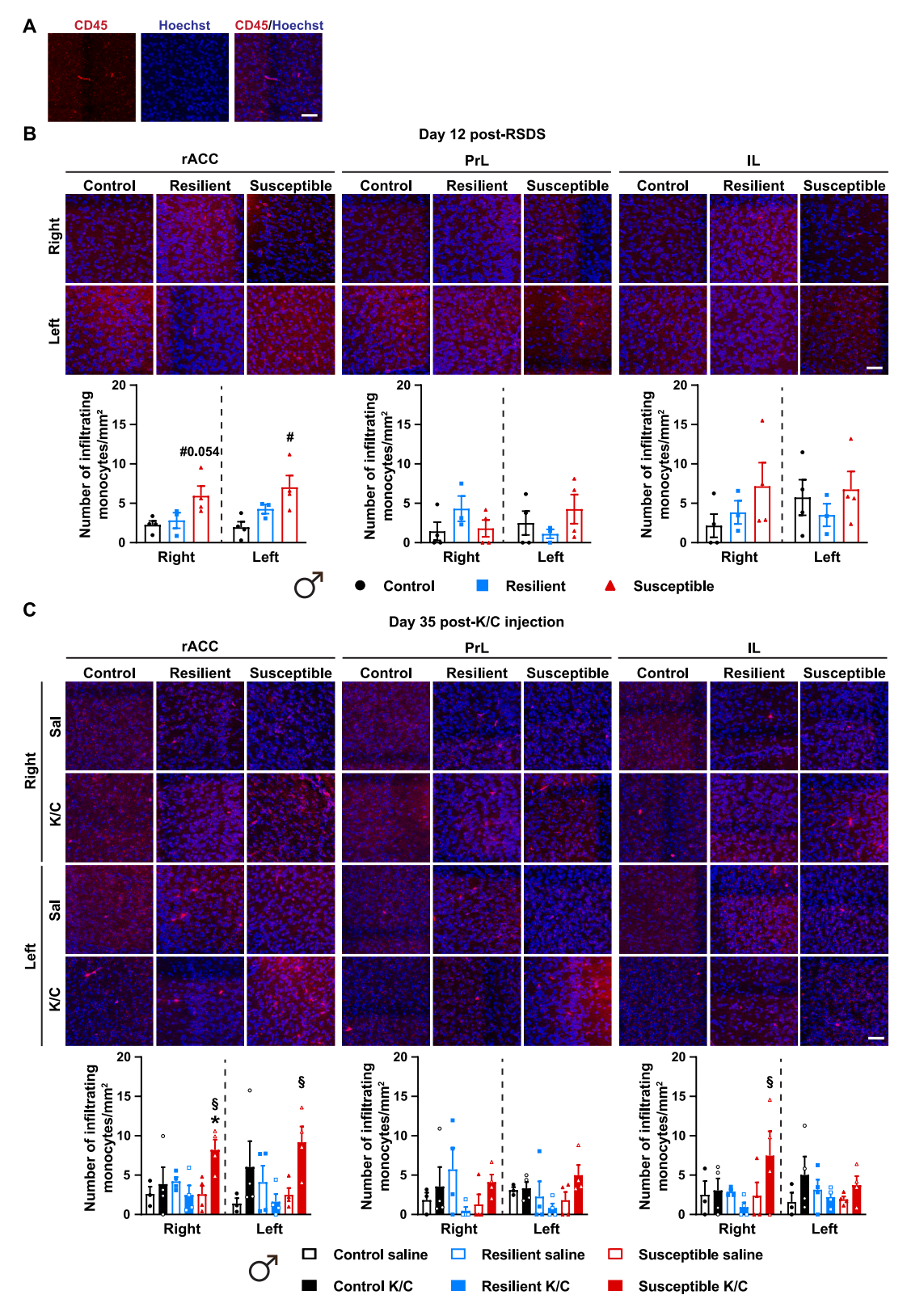


Fig. 7. Monocyte infiltration in the rACC following joint inflammation in susceptible male mice. (A) Representative individual fluorescence and merged images of CD45-positive monocytes (red) and nuclei counterstained with Hoechst (blue) in the rACC. (B-C) Representative images of CD45 immunostaining and nuclear counterstaining with Hoechst and quantification of the number of infiltrating CD45-positive monocytes per area (mm²) in the right and left sides of rACC, PrL and IL at day 12 post-SDS (B, n = 3–4/group) and day 35 post-K/C injection (C, n = 3–5/group). Data are expressed as mean \pm SEM with individual data points representing individual mouse samples. P < 0.05 indicated by * compared to the respective saline group, # compared to the control group; § compared to the resilient group; one-way ANOVA (B) or two-way ANOVA (C) with Tukey-post-hoc-test. See Supplemental Table 1 for further statistical information. Scale bars: 50 μ m. ANOVA, analysis of variance; IL, infralimbic area; K/C, kaolin/carrageenan; PrL, prelimbic area; rACC, rostral anterior cingulate cortex; sal, saline.

compared to resilient K/C) (Fig. 7C).

These results indicated that RSDS induced transient changes in microglia expression in rACC, PrL and IL in both resilient and susceptible male mice, which coincided with the selective monocyte infiltration of rACC specifically in susceptible male mice. In contrast, K/C promoted changes in these markers only in susceptible male mice at the late stage post-injection, suggesting the potential involvement of microglia- and monocyte-associated neuroinflammatory mechanisms in the aggravated pain of these mice following joint inflammation.

Next, we investigated whether the changes in microglia expression and monocyte infiltration in the rACC of male mice were associated with alterations of neuronal activity, by staining for Δ FosB as a marker of sustained neuronal activation directly after RSDS and at day 35 post-K/C injection (Supplemental Fig. 2).

RSDS induced a decrease of neuronal activity of rACC in resilient mice at day 12 post-SDS, indicated by a lower $\Delta FosB$ -positive cell count on both sides of rACC (Supplemental Fig. 2A). In contrast, susceptible mice showed a trend towards an upregulation (Supplemental Fig. 2A). At day 35 post-injection, $\Delta FosB$ -positive cell counts were comparable between resilient and control saline mice, but significantly increased in susceptible saline mice in the left rACC (Supplemental Fig. 2B). K/C injection did not have a major effect on rACC neuronal activity in control and resilient mice, but, interestingly, susceptible K/C mice showed significantly lower $\Delta FosB$ -positive cells in the right and left rACC compared to susceptible saline mice (Supplemental Fig. 2B).

This indicated that RSDS promoted a short-lasting deactivation of rACC in resilient male mice but had long-term effects in susceptible male mice, promoting a higher neuronal activation of the left rACC, which was completely reverted by K/C injection. This compensatory change might have a potential role in pain modulation.

3.7. No major changes in blood cell frequency, rACC microgliosis and monocyte infiltration following RSDS and joint inflammation in female mice

We assessed the levels of circulating immune cells and cytokines, and microglial and monocyte immunoreactivity in the rACC of female mice to further investigate potential sex differences in these immunological parameters following RSDS and joint inflammation.

No changes in the different blood immune cells were found at day 12 post-RSDS or days 5 and 35 post-K/C in female mice (Fig. 8A, Supplemental Table 5), except a significant decrease of the eosinophil frequency in both resilient and susceptible mice compared to controls at day 12 post-RSDS (Fig. 8A). We also analyzed in female mice the cytokines which were mainly regulated in males and found a different pattern of changes (Supplemental Table 6). At day 12 post-RSDS, IL-27, IFN-β and MCP-1 significantly decreased in resilient and susceptible mice, whereas IL-23 and TNF- α were only reduced in susceptible versus control mice (Supplemental Table 6). At day 5 post-K/C, IFN-β was significantly increased in control K/C compared to control saline and both resilient and susceptible K/C mice (Supplemental Table 6). At this time-point, IL-1 β levels were also lower in resilient and susceptible K/C groups than in control K/C group, and IL-23 and IL-27 were lower in resilient K/C compared to resilient saline and control K/C, respectively (Supplemental Table 6). Additionally, at day 35 post-K/C, control K/C mice showed higher levels of IL-10 and IL-12 than control saline and both resilient and susceptible K/C mice (Supplemental Table 6).

At the ipsilateral joint level, neutrophil density was increased in the synovium of susceptible K/C female mice compared to susceptible saline, and to control and resilient K/C mice, for which the neutrophil density was similar to that of their respective saline groups (Fig. 8B). In contrast, macrophage density was increased in the synovium of all K/C control, resilient and susceptible groups compared to their respective saline groups and was significantly higher in susceptible K/C mice compared to both control and resilient K/C mice (Fig. 8C).

Conversely, microglia expression (Fig. 8D) and the number of CD45

positive cells (Fig. 8E) in both right and left sides of the rACC were similar in all the female groups, independently of the stress phenotype and injection.

Taken together, these results indicated that, besides similar alterations in neutrophil and macrophage densities at the joint level, female mice did not show any changes observed in male mice in any of the immune cells and cytokines analyzed in the blood, nor microgliosis or infiltration of monocytes in the rACC.

3.8. Early phase depletion of Ly6C^{high} monocytes abrogated mechanical hypersensitivity of susceptible male mice at the late arthritis stage

We next examined the effect of depleting blood Ly6C^{high} monocytes during the early phase of arthritis in male mice to investigate the functional role of these cells in the development and course of the behavioral alterations associated with RSDS and arthritis in these mice. Following RSDS and starting the day before arthritis induction, we daily injected the mice with the rat anti-mouse CCR2 antibody MC-21 or its IgG isotype control for five days (Fig. 9A). CCR2 is the receptor for CCL2, which is expressed by Ly6C^{high} but not Ly6C^{low} monocytes, and it is necessary for Ly6C^{high} monocyte recruitment from bone marrow (Brühl et al., 2007). All arthritic (K/C) control, susceptible and resilient mice were tested. Control and susceptible groups were represented in Fig. 9 (see Supplemental Fig. 3 for resilient groups).

One day after the end of the antibody treatment (day 4 post-K/C), we observed a robust reduction of blood Ly6C^{high} monocytes frequency in all mice treated with MC-21 compared to IgG (Fig. 9B, Supplemental Fig. 3A, Supplemental Table 7). Susceptible and resilient mice treated with IgG presented also lower Ly6C^{high} monocytes frequency than IgG treated controls (Fig. 9B, Supplemental Table 7). Moreover, NK cell frequency was reduced in susceptible and resilient mice and neutrophil frequency increased only in susceptible mice treated with MC-21 compared to IgG treatment, as a possible compensatory effect. In contrast, the other analyzed cell types were unaffected (Supplemental Table 7). IL-6 blood levels after MC-21 treatment were also increased in controls, as previously reported (Brühl et al., 2007), but decreased in susceptible mice (Supplemental Table 8).

Antibody treatment did not affect the development of mechanical hypersensitivity following arthritis induction (Fig. 9C, Supplemental Fig. 3B). Both control and susceptible K/C groups treated with either MC-21 or IgG displayed similarly reduced 60 % response thresholds at the ipsilateral hindpaw on day 1 and 5 post-K/C injection compared to basal and post-RSDS time-points (Fig. 9C). The response frequencies after the treatment (day 5 post-K/C) were also similar between groups, except for increased response frequency to filament 0.16 g in susceptible IgG compared to control IgG mice (Fig. 9C).

The K/C-induced ipsilateral hypersensitivity in both IgG and MC21 control groups decreased by day 25 as compared to the susceptible groups and returned to pre-injection values at day 34, same as for resilient groups (Fig. 9C, Supplemental Fig. 3B). Interestingly, mechanical hypersensitivity recovered at day 34 in susceptible mice only in those treated with MC-21 (Fig. 9C). In contrast, susceptible IgG mice still displayed lower 60 % response threshold and higher response frequency at this time-point in comparison with control IgG and susceptible MC-21 treated mice (Fig. 9C).

At day 35 post-K/C, MC-21 control mice displayed lower NK cell (vs. IgG controls) and higher eosinophil (vs. IgG control and MC-21 stress groups) and Ly6C^{high} cell frequencies (vs. MC-21 stress groups), despite the absence of behavioral differences between IgG and MC-21 treated control mice (Supplemental Table 7). In contrast, MC-21 treated susceptible mice showed increased B cell and decreased Ly6C^{low} cell frequencies compared to the respective control and resilient groups (Supplemental Table 7) and decreased blood levels of IL-12 compared to IgG susceptible mice at this latest time-point (Supplemental Table 8).

At the joint level (day 35 post-K/C), the density of synovial neutrophils was higher in susceptible mice compared to controls without

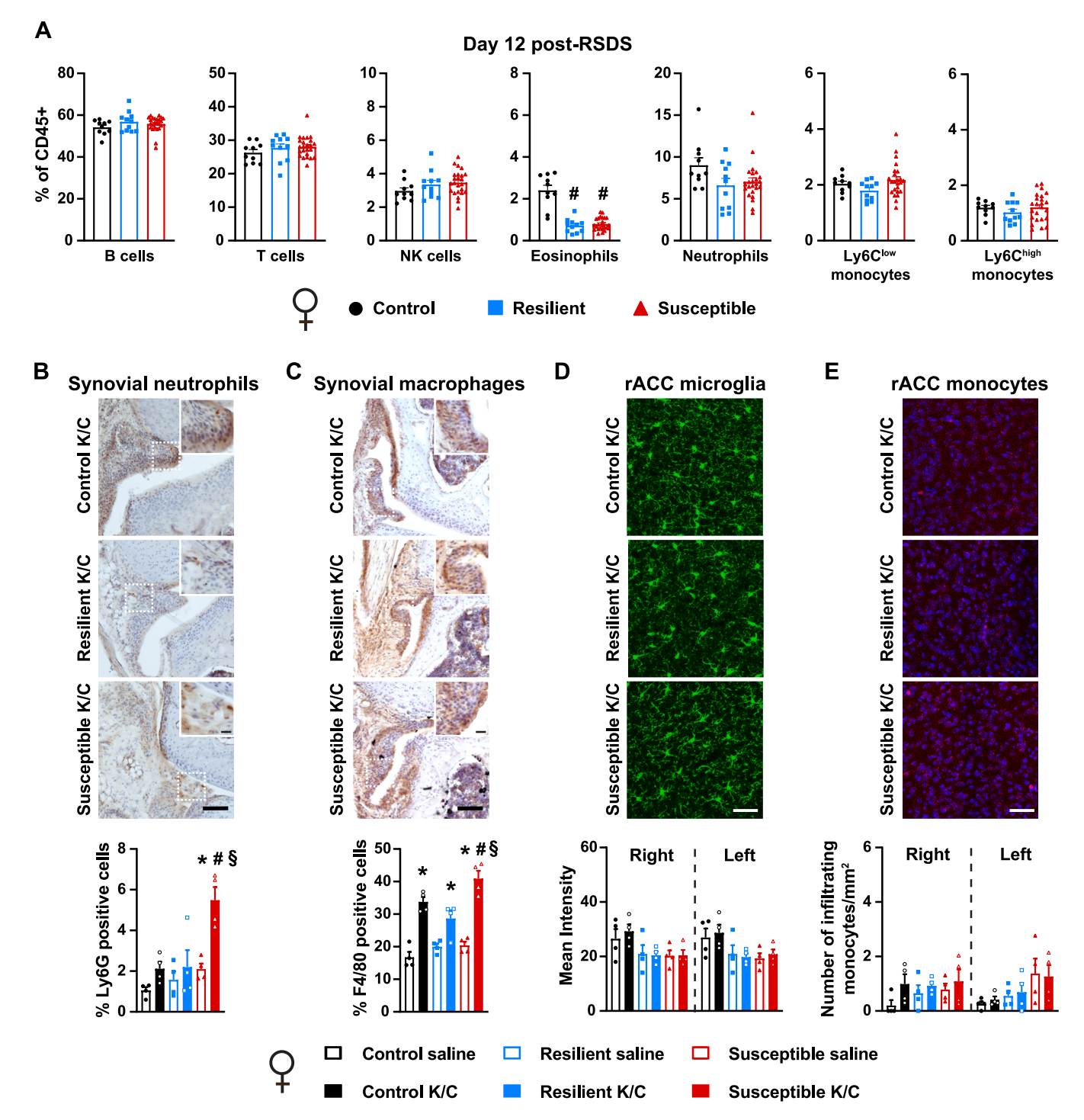
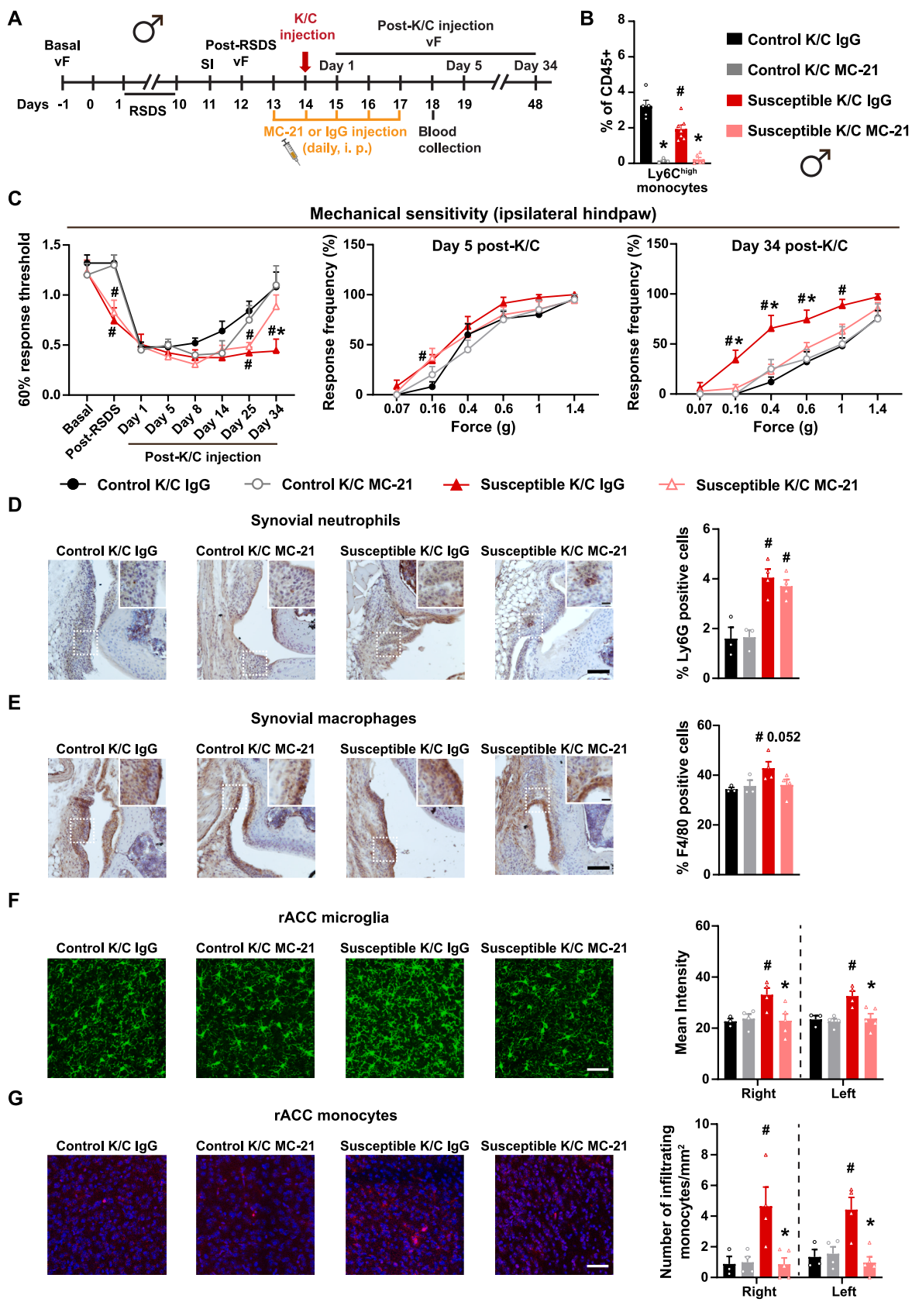


Fig. 8. Absence of major changes in blood cell frequency, rACC microgliosis and monocyte infiltration in susceptible female mice. (A) Relative frequencies of B cells, T cells, NK cells, eosinophils, neutrophils, Ly6C^{low} and Ly6C^{high} monocytes, calculated as the percentage of total CD45+ cells in peripheral blood at day 12 post-RSDS (n=10-24/group). Representative images (only K/C groups) and quantification (all groups) of right knee joint coronal sections at day 35 post-K/C stained with (B) Ly6G marker to measure synovial neutrophil density and (C) F4/80 marker to measure synovial macrophage density (n=4/group). Representative images (only K/C groups) and quantification (all groups) of (D) Iba-1 immunostaining (mean intensity) and (E) number of infiltrating CD45-positive monocytes per area (mm²) in the right and left sides of rACC at day 35 post-K/C injection (n=4/group). Data are expressed as mean \pm SEM with individual data points representing individual mice. P < 0.05 indicated by * compared to the respective saline group, # compared to the control group, § compared to the resilient group; one-way ANOVA (A) or two-way ANOVA (B-E) with Tukey-post-hoc-test. See Supplemental Table 1 for further statistical information. Scale bar: 100 μ m in (B) and (C), 200 μ m in magnified images in (B) and (C), 50 μ m in (D) and (E). ANOVA, analysis of variance; K/C, kaolin/carrageenan; NK, natural killer cells; rACC, rostral anterior cingulate cortex; RSDS, repetitive social defeat stress.



(caption on next page)

Fig. 9. Early phase depletion of Ly6C^{high} monocytes abrogated the mechanical hypersensitivity of susceptible male mice at the late arthritis stage. (A) Scheme of the experimental protocol. After basal vF measurements, RSDS was applied for ten days, followed by the SI test and post-RSDS vF measurements. The antibody treatment (MC-21 or control IgG, i.p.) started one day before arthritis induction (intra-articular K/C injection) and lasted 5 days (from day 13 to day 17), followed by blood collection on day 18 for FACS analysis. Additional vF measurements were taken at different post-K/C injection time points. (B) Relative frequencies of Ly6C^{high} monocytes, calculated as the percentage of total CD45 + cells in peripheral blood at day 18 post-RSDS (n = 4–7/group). (C) Mechanical sensitivity towards graded vF filaments shown as 60 % response threshold over different time points (left panel) and response frequency to individual vF filaments at day 5 (middle panel) and day 34 post-K/C (right panel) at the ipsilateral hindpaw (n = 4–7/group). Representative images and quantification of right knee joint coronal sections at day 35 post-K/C stained with (D) Ly6G marker to measure synovial neutrophil density and (E) F4/80 marker to measure synovial macrophage density (n = 3–4/group). Representative images and quantification of (F) Iba-1 immunostaining (mean intensity) and (G) number of infiltrating CD45-positive monocytes per area (mm²) in the right and left sides of rACC at day 35 post-K/C injection (n = 3–5/group). Data are expressed as mean \pm SEM with individual data points representing individual mice. P < 0.05 indicated by * compared to the respective IgG group, # compared to the control group; two-way ANOVA (B, D-G) or two-way repeated measure ANOVA (C) with Tukey-post-hoc-test. See Supplemental Table 1 for further statistical information. Scale bar: 100 μ m in (D) and (E), 200 μ m in magnified images in (D) and (E), 50 μ m in (F) and (G). ANOVA, analysis of variance; K/C, kaolin/carrageenan; rACC, rostral

significant changes by MC-21 treatment (Fig. 9D). Synovial macrophages were higher in susceptible mice than in controls (Fig. 9E). MC-21 treatment reduced the number of synovial macrophages in susceptible mice but not in controls (Fig. 9E).

Interestingly, microglia density and monocyte infiltration in the right and left sides of rACC were higher in susceptible mice compared to controls (Fig. 9F and G). Treatment with MC-21 significantly reduced both parameters in susceptible mice but not in controls (Fig. 9F and G).

No changes were observed at the joint or rACC levels between IgG and MC-21 treated resilient mice (Supplemental Fig. 3C, D, E, F).

Thus, Ly6C $^{\rm high}$ monocyte depletion with MC-21 treatment during the initiation phase of arthritis abrogated the mechanical hypersensitivity of susceptible male mice at the late arthritis stage and reduced the associated changes in microglia and monocyte infiltration in the rACC of these mice.

4. Discussion

This study showed that arthritis-associated hypersensitivity was exacerbated and prolonged in stress susceptible male mice, involving peripheral and central inflammatory responses. Ly6C high monocytes had a crucial role in the long-lasting behavioral and immunological alterations of susceptible male mice. Their depletion in the blood during the initiation phase of arthritis promoted pain recovery at the late arthritis stage, coinciding with the abolishment of the central inflammatory responses. In contrast, the persistence of arthritis-induced pain in susceptible female mice was not associated with major changes in circulating immune cells nor central microglial or monocyte alterations. This suggested different mechanisms underlying the stress-induced chronicity of inflammatory joint pain in male and female mice.

4.1. RSDS model and behavior in male mice

RSDS has been extensively used for its high face validity, recapitulating many stress-induced immune and behavioral outcomes (Cathomas et al., 2019; Golden et al., 2011; Scarpa et al., 2020; Weber et al., 2017). Here, resilient and susceptible male mice displayed typical changes of chronic stress exposure, i.e., increased despair behavior and FCM levels. In contrast, only susceptible mice developed social avoidance, anhedonia and reliable anxiety, similar to previous studies (Bravo-Tobar et al., 2021; Krishnan et al., 2007; Menard et al., 2017; Okamura et al., 2022). While social avoidance and anhedonia have been reliably associated with RSDS susceptibility as correlates of depression (Cathomas et al., 2019; Krishnan et al., 2007), assessing anxiety and despair behaviors has provided less consistent results (Bravo-Tobar et al., 2021; Krishnan et al., 2007; Li et al., 2019; Murra et al., 2022; Okamura et al., 2022; W. Wang et al., 2022; Xu et al., 2021).

Additionally, both stress groups showed persistent mechanical but not thermal hypersensitivity, in agreement with previous studies (Marco Pagliusi et al., 2020; Pagliusi et al., 2018; Piardi et al., 2020; Sawicki et al., 2018, 2019; Xu et al., 2021). RSDS-induced hypersensitivity was

reported to be mediated by neuroinflammation in the spinal cord and brain (Bravo-Tobar et al., 2021; Piardi et al., 2020; Sawicki et al., 2018, 2019; W. Wang et al., 2022).

Susceptible and resilient mice also displayed comparable short-lasting reductions in voluntary wheel running activity, as previously reported (M. Pagliusi et al., 2020). In contrast, susceptible mice showed lower performances than control and resilient mice following wheel running training over several days or on an accelerating rotarod (Gellner et al., 2022; M. Pagliusi et al., 2020). This impairment was associated with disrupted dendritic spine dynamics and neuroinflammation in the motor cortex (Gellner et al., 2022). We avoided training because it prevents RSDS-induced social avoidance and mechanical hypersensitivity (M. Pagliusi et al., 2020) and promotes resilience (Mul et al., 2018).

Although differences in gait patterns between depressed and healthy individuals were described (Adolph et al., 2021; Wang et al., 2021), RSDS did not affect gait parameters in our study.

4.2. RSDS effects on arthritis in male mice

The intra-articular K/C injection, mimicking the acute inflammatory phase of osteoarthritis (Neugebauer, 2007; Neugebauer et al., 2007), induced transient joint swelling, mechanical and thermal hypersensitivity lasting longer than alterations in gait and running activity. Similar temporal alterations were observed in other inflammatory models (Nees et al., 2023; Pitzer et al., 2016).

RSDS prolonged mechanical hypersensitivity following plantar mild inflammation (Piardi et al., 2020) or incision (W. Wang et al., 2022) and lumbar disk herniation (Yomogida et al., 2020), without distinguishing between resilient and susceptible mice. In our study, susceptible K/C mice displayed exacerbated and prolonged mechanical hypersensitivity and gait alterations compared to control and resilient mice. Although resilient K/C mice showed similar mechanical hypersensitivity as controls, their gait patterns were minimally affected compared to control and susceptible mice. This suggested that resilient mice could perceive less pain/ discomfort from touching the floor with the inflamed hind limb while walking. We did not observe further impairment of voluntary wheel running activity after arthritis induction in RSDS groups, which could have been influenced by the motivational/rewarding effects of this task (Greenwood and Fleshner, 2019).

In humans, stress vulnerability factors like worrying predicted the course of pain and functional disability associated with arthritis (Evers et al., 2014). In contrast, resilient factors were associated with reduced pain severity (Johnson et al., 2019; Musich et al., 2019).

Consistent with the poor correlation between structural pathology and pain experienced by osteoarthritis patients (Astephen Wilson et al., 2017; Finan et al., 2013), the distinct pain behavior between control, susceptible and resilient mice was not related to joint swelling, cartilage damage or global synovial inflammation levels. This discrepancy supports the idea that arthritic pain is not just the result of local inflammation but other systemic or CNS-related mechanisms play a role.

4.3. RSDS and arthritis effects on circulating immune cells in male mice

Repeated stress exposure activates the HPAA leading to increased release of corticosterone (Raison et al., 2006), in agreement with the increased FCM levels measured at the end of RSDS in males. Prolonged corticosterone release induces glucocorticoid resistance, causing increased recruitment of peripheral myeloid cells and pro-inflammatory cytokine release (Cathomas et al., 2019; Davis et al., 2009; Hodes et al., 2014; Niraula et al., 2018; Raison et al., 2006) and shifting immune signaling toward a pro-inflammatory state (Weber et al., 2017). Here, RSDS reduced B and T cells and increased neutrophil and Ly6Chigh monocytes in resilient and susceptible mice, as previously shown (Ishikawa et al., 2020; Pfau et al., 2019).

Importantly, we showed that these changes were transient and lasted longer in susceptible than in resilient mice. The protracted reduction of B and T cells only in susceptible mice in our study matched the finding that lymphocytes confer resilience (Brachman et al., 2015). Notably, while neutrophils persisted increased in susceptible, they decreased in resilient mice at the end of the observation period. Higher neutrophil levels were also found one week after the end of a shorter RSDS version and were higher in the BALB/c susceptible mouse strain than in C57BL6/N (Ishikawa et al., 2020). The role of neutrophils in depression is emerging, as systemic infection promotes neutrophils migration to the brain and causes depressive-like behaviors (Aguliar-Valles et al., 2013; Kong et al., 2021). Also, monocytes are critical in stress-induced depressive disorders and are subjected to a transient regulation (Lehmann et al., 2022; Weber et al., 2017).

Joint inflammation induced further changes in blood cell frequency, with neutrophils and Ly6C^{high} monocytes being the most differentially modulated between control and RSDS groups. K/C injection did not cause significant changes in control mice, except a decrease of neutrophil frequency at day 35, which might correspond to a compensatory mechanism to potentially reduce their synovium infiltration, contributing to pain recovery. In contrast, the post-K/C injection changes of resilient mice in B and T cells, neutrophils and Ly6C^{high} monocytes corresponded to the transient changes that these mice showed before arthritis induction (end of RSDS). This suggested that the pathways regulating these cells remained primed in resilient mice and were reactivated by arthritis induction.

Interestingly, susceptible K/C mice had significantly lower NK cell frequency at days 5 and 35 post-KC, in agreement with previous studies showing decreased or fluctuating NK cell levels in depressed individuals and arthritis, respectively (Ader et al., 1995; Wu et al., 2022). Higher Ly6C^{high} monocyte frequency in susceptible K/C at day 5 post-injection might contribute to their exacerbated pain. Indeed, Ly6Chigh monocytes are recruited into the inflamed joint in response to chemokines and differentiate in inflammatory macrophages (Cremers et al., 2017). These cells release various mediators, leading to increased nociceptor excitability and hypersensitivity to pain stimuli (Geraghty et al., 2021). The Ly6Chigh cell increase at day 5 post-K/C coincided with higher Ly6Clow levels in susceptible K/C, possibly as a compensatory mechanism promoting anti-inflammatory macrophage differentiation. However, the early phase depletion of Ly6Chigh cells did not affect the development of mechanical hypersensitivity or the response thresholds, indicating that these cells are not the only ones involved at this stage. Moreover, this coincided in susceptible mice with other compensatory changes occurring in circulating NK cells and neutrophils, which could have participated in maintaining the hypersensitivity (Ghasemlou et al., 2015). In contrast, monocyte depletion promoted pain recovery at the late stage in these mice and was associated with Ly6Clow decrease once the resolution had occurred.

4.4. RSDS and arthritis effects on circulating cytokines in male mice

The immune system communicates with the CNS via cytokines released by activated immune cells, thereby influencing behavior (Ader

et al., 1995). Increased C-reactive protein and pro-inflammatory cytokines levels were described in depressed patients (Himmerich et al., 2019). We showed that the levels of several cytokines, including IL-6, IL-10, IL-12, IL-17A and IL-27, were altered following RSDS and were differentially regulated over time. All here reported cytokines have been implicated in stress response and depression (Elgellaie et al., 2023; Elkhatib et al., 2022; Harsanyi et al., 2023; Himmerich et al., 2019; Serna-Rodríguez et al., 2022). Among these, IL-6 is a strong indicator of stress and stress-induced psychiatric disorders, is elevated in depressive patients and predicts RSDS susceptibility when measured before RSDS (Gallagher et al., 2019; Harsanyi et al., 2023; Hodes et al., 2014; Nasca et al., 2019). However, IL-6 is an acute-phase protein regulated by the HPAA. Its induction is corticosterone-dependent (Niraula et al., 2018) and, therefore, was equally increased in resilient and susceptible mice immediately after RSDS, but not later. IL-17A levels, although similarly increased at the beginning in both RSDS groups, were higher at the latest time-point only in susceptible mice. High circulating IL-17A levels represent a clinical marker for depressed patients, especially the nonresponders to antidepressant therapy (Harsanyi et al., 2023). IL-17 induces neutrophil expansion and mobilization (Ishikawa et al., 2020), in agreement with the higher neutrophil blood frequency in susceptible mice at late stages. The higher IL-17 levels in susceptible mice matched the simultaneous lower IL-27 levels. Accordingly, IL-27 can inhibit the generation of IL-17-producing T cells (T_H17) (Stumhofer et al., 2006). Notably, IL-17 and T_H17 cells have been heavily implicated in depression and inflammatory or autoimmune diseases (Elkhatib et al., 2022; Kim et al., 2021; H. Wang et al., 2022). Interestingly, the antiinflammatory IL-10 was consistently higher in resilient mice across time as an inherent compensatory immune response to stress, in agreement with the reduced or increased levels of this cytokine in depressed patients or after anti-depressant treatment, respectively (Harsanyi et al., 2023; Serna-Rodríguez et al., 2022). Moreover, IL-10 is post-transcriptionally regulated by the monocyte-derived micro-RNA106b \sim 25 associated with resilience (Pfau et al., 2019). Its levels are also inversely correlated with osteoarthritis disease (Molnar et al., 2021).

Besides regulating the neuroendocrine function by interacting with the HPAA, pro-inflammatory cytokines control neurotransmitter metabolism and signaling (Himmerich et al., 2019), thereby influencing emotional-like behavior and pain, in agreement with the hypersensitivity shown by the RSDS mice. Pro-inflammatory cytokines directly activate and sensitize nociceptors, and modulate excitatory synaptic transmission at central terminals (Sawicki et al., 2020). The RSDS-induced inflammatory environment, especially in susceptible mice, could have further switched nociceptor properties, a process called hyperalgesic priming (Piardi et al., 2020), rendering them more sensitive to subsequent inflammatory insults, which in our case is represented by arthritis induction, leading to exacerbated pain.

Following K/C injection, susceptible mice displayed higher levels of TNF- α , like controls K/C, and IL-6, which can be released by monocytes (Hodes et al., 2014), in agreement with the decreased IL-6 levels observed after monocyte depletion in these mice. Both cytokines are known modulators of nociceptor activity and pain sensitization and are highly involved in arthritis (McInnes and Schett, 2007; Molnar et al., 2021). Their high blood concentration predicted disease severity (Molnar et al., 2021) and was found in early osteoarthritis stages (Alonso-Castro et al., 2015; Barker et al., 2014), consistent with our study. Moreover, pain patients treated with inhibitors of IL-6 demonstrated reduced pain and improved mood symptoms (Sawicki et al., 2020).

Interestingly, at the late arthritis stage, susceptible K/C also showed higher IL-12 and IL-22 levels, and lower IL-27 levels compared to control K/C showing an opposite regulation of these cytokines. IL-12 levels were elevated in arthritis patients with psychiatric comorbidities (Himmerich et al., 2019) and correlated with disease severity (Pope and Shahrara, 2013), consistent with the decreased IL-12 levels observed here after monocyte depletion. Contrary to elevated IL-22 levels in susceptible K/C

mice, no changes in IL-22 concentration were observed in control K/C or in osteoarthritis patients serum (Molnar et al., 2021). Instead, the opposite regulation of IL-27 in control and susceptible K/C mice suggests that its increase might be associated with pain recovery at the late stage. IL-27 limits neutrophil recruitment, reduces IL-6 and IL-12 secretion (Jafarzadeh et al., 2020), and positively correlates with macrophage presence in arthritis synovium (Hsueh et al., 2021), in line with the observed changes at day 35 post-K/C in control mice.

4.5. RSDS and arthritis effects on synovial fluid and tissue in male mice

Blood cell and cytokine changes were not reflected at the synovial fluid level at the late arthritis stage. Alterations in synovial fluid immune cells recovered one week after arthritis induction in another model (Benigni et al., 2017). The increased density of synovial neutrophils and macrophages in susceptible mice at the late arthritis stage may contribute to the prolonged hypersensitivity. Synergistic roles of macrophages and neutrophils in human osteoarthritis severity and progression were described (Haraden et al., 2019; Hsueh et al., 2021). However, few clinical and rodent studies have addressed how macrophages and neutrophils influence pain severity (Bai et al., 2022; Geraghty et al., 2021; Hsueh et al., 2021; Raghu et al., 2017; Valdrighi et al., 2022). Macrophages, neutrophils and nociceptors mutually influence each other by releasing different mediators (e.g., cytokines, chemokines, alarmins, elastases, neuropeptides), maintaining a pro-inflammatory milieu (Valdrighi et al., 2022).

While macrophages were localized to arthritic synovial tissue and fluid, neutrophils were predominantly localized to synovial fluid (Hsueh et al., 2021). Studies in other arthritis models and humans demonstrated that macrophages are derived from infiltrating monocytes (Cremers et al., 2017; Raghu et al., 2017), although tissue-resident macrophages also expand during inflammation resolution (Geraghty et al., 2021). In agreement, macrophage synovial density returned to control levels in susceptible K/C mice after monocyte depletion, whereas neutrophil density was not affected, as previously shown (Brühl et al., 2007).

The immune regulation in our model combining RSDS and arthritis was not associated with FCM changes. Accordingly, no consistent alterations in HPAA were found in arthritis patients exposed to stress (Davis et al., 2009; De Brouwer et al., 2014; Evers et al., 2014) and HPAA activity returned to homeostatic levels at the end of RSDS (Lehmann et al., 2013; Weber et al., 2017).

4.6. RSDS and arthritis effects on the brain in male mice

Microglia are the first immune cells reacting to stress in the CNS, expressing β-adrenergic and glucocorticoid receptors (Calcia et al., 2016). Microglia activation contributes to neuroinflammation, particularly within stress-reactive brain regions (frontal cortex, hypothalamus, amygdala, hippocampus) and spinal cord, the first relay for pain transmission in the CNS (Niraula et al., 2018; Sawicki et al., 2019; Weber et al., 2017). Neuroinflammation influences the behavioral response to stress in animals (McKim et al., 2018; Sawicki et al., 2019; Weber et al., 2017) and represents a core feature in human depression. Brainactivated microglia and elevated pro-inflammatory cytokines in the cerebrospinal fluid were reported in depressed patients (Setiawan et al., 2015; Weber et al., 2017). RSDS-induced neuroinflammation is characterized by increased cytokines (IL-1 β , IL-6, TNF- α) and chemokines (CCL2/MCP-1) release, reduced fractalkine/CX3CL1 ligand and receptor expression and upregulation of surface adhesion molecules (CD14, TLRs, and CD86) (Weber et al., 2017). Stress "primes" microglia, as they produce an exaggerated pro-inflammatory response to subsequent immune challenges (Weber et al., 2017; Wohleb et al., 2015). This is consistent with a potentially stronger or longer-lasting priming effect in susceptible than resilient mice, in line with the increased microglia expression and monocyte brain infiltration found only in susceptible mice at the late arthritis stage.

This is the first study showing monocyte rACC infiltration following joint inflammation in susceptible mice very long time after RSDS exposure. The ACC is particularly responsive to stress and pain, also during arthritis (Abe et al., 2022; Kummer et al., 2020; Malange et al., 2022; Süß et al., 2020).

Previous studies demonstrated that RSDS promoted the recruitment of peripherally-derived Ly6Chigh monocytes to stress-responsive prefrontal brain regions, especially rACC, where they transformed into macrophages and propagated neuroinflammatory signaling by interacting with microglia to promote anxiety-like behavior (McKim et al., 2018; Nie et al., 2018; Niraula et al., 2018; Weber et al., 2017; Wohleb et al., 2013). Leukocyte trafficking into the brain, but not the spinal cord (Sawicki et al., 2019), was attributed to cerebrovascular damage (Cathomas et al., 2019; Lehmann et al., 2022) or active recruitment to stress-responsive regions by neuroinflammatory mediators and endothelial adhesion molecules (Weber et al., 2017; Wohleb et al., 2015, 2013). Notably, monocyte recruitment was transient and was corticosterone- and microglia-dependent, resolving twenty-four days after RSDS, together with neuroinflammation and anxiety-like behavior (McKim et al., 2018; Niraula et al., 2018; Wohleb et al., 2015, 2014). Sub-threshold stress could re-establish it (Wohleb et al., 2015, 2014). A similar effect might have been mediated by arthritis induction in susceptible mice by prolonging microglia activation and monocyte infiltration. Accordingly, Ly6Chigh monocyte depletion during the initiation phase of arthritis abolished the late stage rACC microgliosis and monocyte infiltration, coinciding with pain recovery in susceptible

The neuroinflammatory status in rACC might have affected the neuronal pain circuits and facilitated pain persistence in susceptible mice. Microglial activation and monocyte infiltration spatially coincided with reduced neuronal activation in susceptible mice at the late arthritis stage. Similarly, combining forced swimming stress and paw inflammation decreased neuronal activation in the insular cortex and was associated with enhanced mechanical hypersensitivity (Imbe and Kimura, 2015). Decreased neuronal activation in the ACC was also observed following systemic inflammation and was associated with microglia activation (He et al., 2023). This potentially contributed to ACC dysfunction and influenced pain behavioral responses by regulating excitatory neuronal transmission (Vialou et al., 2014, 2010).

4.7. RSDS effects on arthritis in female mice

Despite similar emotional-like behavior following RSDS in female and male mice, as previously shown (Harris et al., 2018), our findings in female mice revealed differences in patterns of mechanical sensitivity, FCM levels, immune cell recruitment, cytokine production, and absence of microglia-mediated neuroinflammatory response in the brain compared to males. The fact that we did not observe a long-lasting effect of RSDS on mechanical sensitivity, nor increased pain severity following arthritis induction (only pain persistence at the late stage) in susceptible female mice compared to controls, could have different possible explanations. First, control females were also physically separated from their cage mates, although not receiving the defeat protocol, and females are more sensitive to social isolation than males (Senst et al., 2016), possibly contributing to the similar mechanical sensitivity in stressed and nonstressed groups. Secondly, defeated female mice can perceive or receive the attacks from a male mouse differently than males, because of sexual-related physiology/ behavior due to the presence of male urine and male aggressor (Harris et al., 2018). These differences limit the direct comparison of males and females in this model and may contribute to different cellular and molecular mechanisms underlying the behavioral responses. This resulted in the absence of the typical immune cell and cytokine profiles found in the blood of males following RSDS or in an alternative, more intense, RSDS female model (Yin et al., 2019). Unexpectedly, we observed solely circulating eosinophil reduction in all stressed females after RSDS. Eosinopenia has been associated

with diverse kinds of stress in women (Oyster, 1980). No other changes following arthritis induction were observed in females, except for higher infiltration of neutrophils and macrophages in the inflamed synovium of susceptible females compared to controls, similar to males. We did not directly compare males and females. However, sex differences are known in pain manifestation, immune cells, molecular composition at the joint level, and pain pathways under inflammatory states in patients and rodents (Kim and Kim, 2020; Valdrighi et al., 2022).

The absence of microglia/ monocyte-related changes in the CNS suggests that alternative pathways responsible for pain persistence might exist in susceptible females. Previously, RSDS-induced prolonged post-surgical pain was observed in both males and females, but it was mediated by spinal microglial activation only in males (W. Wang et al., 2022). In accordance, microglia-specific genes were downregulated in women and upregulated in men with depression (Seney et al., 2018). Previous studies demonstrated that mechanical hypersensitivity in female mice is mediated by T-cell infiltration rather than microglia (Sorge et al., 2015). Although the cell and cytokine profiles in female blood did not point out a specific regulation of T cells in our study, we cannot exclude their potential involvement in the behavioral responses of susceptible female mice with arthritis. Mechanical pain in females was also demonstrated to be mediated through macrophage-neuron crosstalk via the IL-23/IL-17/TRPV1 axis in dorsal root ganglia (Valdrighi et al., 2022).

5. Conclusions

This study advanced our understanding of how peripheral and central immune processes participate in stress-induced behavioral and neurochemical alterations.

Released immune cells, especially Ly6Chigh monocytes, and cytokines are potential key mediators of the persistent arthritis-associated hypersensitivity in stress susceptible male mice, as they regulate the inflammatory responses locally at the joint and centrally in the rACC. However, how all these factors interact with each other remains to be elucidated. Notably, female mice presented different behavioral and immune regulations than males, and, therefore, investigating the specific cellular and molecular mechanisms involved in females deserves further investigation. Nevertheless, our findings highlight potential advantages of targeting monocytes to prevent chronic inflammatory pain in specific patient populations, particularly those susceptible to chronic stress.

CRediT authorship contribution statement

Carmen La Porta: Writing – review & editing, Writing – original draft, Validation, Supervision, Project administration, Methodology, Investigation, Formal analysis, Data curation, Conceptualization. Thomas Plum: Writing – review & editing, Methodology, Formal analysis. Rupert Palme: Writing – review & editing, Methodology, Formal analysis. Matthias Mack: Writing – review & editing, Resources, Methodology. Anke Tappe-Theodor: Writing – review & editing, Writing – original draft, Supervision, Resources, Project administration, Methodology, Investigation, Funding acquisition, Formal analysis, Data curation, Conceptualization.

Declaration of Competing Interest

The authors declare that they have no known competing financial interests or personal relationships that could have appeared to influence the work reported in this paper.

Data availability

Data will be made available on request.

Acknowledgments

This work was funded by a Collaborative Research Center 1158 (SFB1158) grant from the Deutsche Forschungsgemeinschaft (DFG), Germany to A. Tappe-Theodor (project S01).

CLP and ATT conceptualized the study, designed and performed experiments and analyzed data. TP helped designing, performed and analyzed FACS experiments. RP performed the FCM analysis. MM helped designing and discussed the experiments concerning MC-21 antibody treatment. CLP and ATT wrote the manuscript with feedback from all the authors.

The authors thank Julia Speck, Florencia Garrido Charrad, Cecilia Beatriz Berzain Battioni and Edith Klobetz-Rassam for their expert technical help. The work was performed at the Interdisciplinary Neurobehavioral Core (INBC), University of Heidelberg, Germany.

All cartoons were created with BioRender.com.

Appendix A. Supplementary data

Supplementary data to this article can be found online at https://doi.org/10.1016/j.bbi.2024.04.025.

References

- Abe, N., Fujieda, Y., Tha, K.K., Narita, H., Aso, K., Karino, K., Kanda, M., Kono, M., Kato, M., Amengual, O., Atsumi, T., 2022. Aberrant functional connectivity between anterior cingulate cortex and left insula in association with therapeutic response to biologics in inflammatory arthritis. Semin. Arthritis Rheum. 55, 151994 https://doi.org/10.1016/j.semarthrit.2022.151994.
- Ader, R., Cohen, N., Felten, D., 1995. Psychoneuroimmunology: interactions between the nervous system and the immune system. Lancet 345, 99–103. https://doi.org/ 10.1016/S0140-6736(95)90066-7.
- Adolph, D., Tschacher, W., Niemeyer, H., Michalak, J., 2021. Gait Patterns and Mood in Everyday Life: A Comparison Between Depressed Patients and Non-depressed Controls. Cogn. Ther. Res. 45, 1128–1140. https://doi.org/10.1007/s10608-021-10215-7
- Aguliar-Valles, A., Kim, J., Jung, S., Woodside, B., Luheshi, G.N., 2013. Role of brain transmigrating neutrophils in depression-like behavior during systemic infection. Molecular Psychiatry 2013 19:5 19, 599–606. https://doi.org/10.1038/ mp.2013.137.
- Alonso-Castro, A.J., Zavala-Sánchez, M.A., Pérez-Ramos, J., Sánchez-Mendoza, E., Pérez-Gutiérrez, S., 2015. Antinociceptive and anti-arthritic effects of kramecyne. Life Sci. 121, 70–77. https://doi.org/10.1016/j.lfs.2014.11.015.
- American Psychiatric Association (APA), 2013. Diagnostic and Statistical Manual of Mental Disorders (DSM-V). 5th Edition [WWW Document]. DSM Library. URL https://dsm.psychiatryonline.org/doi/book/10.1176/appi.books.9780890425596 (accessed 7.17.23).
- Ängeby Möller, K., Aulin, C., Baharpoor, A., Svensson, C.I., 2020. Pain behaviour assessments by gait and weight bearing in surgically induced osteoarthritis and inflammatory arthritis. Physiol. Behav. 225, 113079 https://doi.org/10.1016/j. physbeh.2020.113079.
- Astephen Wilson, J.L., Stanish, W.D., Hubley-Kozey, C.L., 2017. Asymptomatic and symptomatic individuals with the same radiographic evidence of knee osteoarthritis walk with different knee moments and muscle activity. J. Orthop. Res. 35, 1661–1670. https://doi.org/10.1002/jor.23465.
- Bai, L.-K., Su, Y.-Z., Wang, X.-X., Bai, B., Zhang, C.-Q., Zhang, L.-Y., Zhang, G.-L., 2022. Synovial Macrophages: Past Life, Current Situation, and Application in Inflammatory Arthritis. Front. Immunol. 13, 905356 https://doi.org/10.3389/ fimmu.2022.905356.
- Barker, T., Rogers, V.E., Henriksen, V.T., Aguirre, D., Trawick, R.H., Rasmussen, G.L., Momberger, N.G., 2014. Serum cytokines are increased and circulating micronutrients are not altered in subjects with early compared to advanced knee osteoarthritis. Cytokine 68, 133–136. https://doi.org/10.1016/j.cyto.2014.04.004.
- Benigni, G., Dimitrova, P., Antonangeli, F., Sanseviero, E., Milanova, V., Blom, A., van Lent, P., Morrone, S., Santoni, A., Bernardini, G., 2017. CXCR3/CXCL10 Axis Regulates Neutrophil–NK Cell Cross-Talk Determining the Severity of Experimental Osteoarthritis. J. Immunol. 198, 2115–2124. https://doi.org/10.4049/ immunol.1601350
- Brachman, R.A., Lehmann, M.L., Maric, D., Herkenham, M., 2015. Lymphocytes from chronically stressed mice confer antidepressant-like effects to naive mice. J. Neurosci. 35, 1530–1538. https://doi.org/10.1523/JNEUROSCI.2278-14.2015.
- Bravo-Tobar, I.D., Fernández, P., Sáez, J.C., Dagnino-Subiabre, A., Franklin, T., Mcarthur, D., Reviewed, J.W., Schiavone, S., Aguilar-Valles, A., 2021. Long-term effects of stress resilience: Hippocampal neuroinflammation and behavioral approach in male rats. J. Neurosci. Res. 99, 2493–2510. https://doi.org/10.1002/ JNR.24902.
- Brühl, H., Cihak, J., Plachý, J., Kunz-Schughart, L., Niedermeier, M., Denzel, A., Rodriguez Gomez, M., Talke, Y., Luckow, B., Stangassinger, M., Mack, M., 2007.

- Targeting of Gr-1+, CCR2+ monocytes in collagen-induced arthritis. Arthritis Rheum. 56, 2975–2985. https://doi.org/10.1002/art.22854.
- Calcia, M.A., Bonsall, D.R., Bloomfield, P.S., Selvaraj, S., Barichello, T., Howes, O.D., 2016. Stress and neuroinflammation: A systematic review of the effects of stress on microglia and the implications for mental illness. Psychopharmacology (Berl) 233, 1637–1650. https://doi.org/10.1007/s00213-016-4218-9.
- Cathomas, F., Murrough, J.W., Nestler, E.J., Han, M.H., Russo, S.J., 2019. Neurobiology of Resilience: Interface Between Mind and Body. Biol. Psychiatry 86, 410–420. https://doi.org/10.1016/j.biopsych.2019.04.011.
- Chaney, S., Vergara, R., Qiryaqoz, Z., Suggs, K., Akkouch, A., 2022. The Involvement of Neutrophils in the Pathophysiology and Treatment of Osteoarthritis. Biomedicines 10, 1604. https://doi.org/10.3390/biomedicines10071604.
- Cremers, N.A.J., van den Bosch, M.H.J., van Dalen, S., Di Ceglie, I., Ascone, G., van de Loo, F., Koenders, M., van der Kraan, P., Sloetjes, A., Vogl, T., Roth, J., Geven, E.J. W., Blom, A.B., van Lent, P.L.E.M., 2017. S100A8/A9 increases the mobilization of pro-inflammatory Ly6Chigh monocytes to the synovium during experimental osteoarthritis. Arthritis Res. Ther. 19, 217. https://doi.org/10.1186/s13075-017-1436.6
- Dainese, P., Wyngaert, K.V., De Mits, S., Wittoek, R., Van Ginckel, A., Calders, P., 2022. Association between knee inflammation and knee pain in patients with knee osteoarthritis: a systematic review. Osteoarthr. Cartil. 30, 516–534. https://doi.org/ 10.1016/j.joca.2021.12.003.
- Davis, M.C., Ph. D., Zautra, A.J., Younger, J., Motivala, S.J., Attrep, J., Irwin, M.R., 2009. in Rheumatoid Arthritis: Implications for Fatigue. Brain 22, 24–32.
- De Brouwer, S.J.M., Van Middendorp, H., Stormink, C., Kraaimaat, F.W., Sweep, F.C.G. J., De Jong, E.M.G.J., Schalkwijk, J., Eijsbouts, A., Donders, A.R.T., Van De Kerkhof, P.C.M., Van Riel, P.L.C.M., Evers, A.W.M., 2014. The psychophysiological stress response in psoriasis and rheumatoid arthritis. Br. J. Dermatol. 170, 824–831. https://doi.org/10.1111/bjd.12697.
- Elgellaie, A., Thomas, S.J., Kaelle, J., Bartschi, J., Larkin, T., 2023. Pro-inflammatory cytokines IL-1α, IL-6 and TNF-α in major depressive disorder: Sex-specific associations with psychological symptoms. Eur. J. Neurosci. 57, 1913–1928. https://doi.org/10.1111/ejin.15992.
- Elkhatib, S.K., Moshfegh, C.M., Watson, G.F., Case, A.J., 2020. Peripheral inflammation is strongly linked to elevated zero maze behavior in repeated social defeat stress. Brain Behav. Immun. 90, 279–285. https://doi.org/10.1016/j.bbi.2020.08.031.
- Elkhatib, S.K., Moshfegh, C.M., Watson, G.F., Case, A.J., 2022. T-lymphocyte tyrosine hydroxylase regulates TH17 T-lymphocytes during repeated social defeat stress. Brain Behav. Immun. 104, 18–28. https://doi.org/10.1016/j.bbi.2022.05.007.
- Evers, A.W.M., Verhoeven, E.W.M., Van Middendorp, H., Sweep, F.C.G.J., Kraaimaat, F. W., Donders, A.R.T., Eijsbouts, A.E., Van Laarhoven, A.I.M., De Brouwer, S.J.M., Wirken, L., Radstake, T.R.D.J., Van Riel, P.L.C.M., 2014. Does stress affect the joints? Daily stressors, stress vulnerability, immune and HPA axis activity, and short-term disease and symptom fluctuations in rheumatoid arthritis. Ann. Rheum. Dis. 73, 1683–1688. https://doi.org/10.1136/annrheumdis-2012-203143.
- Finan, P.H., Buenaver, L.F., Bounds, S.C., Hussain, S., Park, R.J., Haque, U.J., Campbell, C.M., Haythornthwaite, J.A., Edwards, R.R., Smith, M.T., 2013. Discordance Between Pain and Radiographic Severity in Knee Osteoarthritis. Arthritis Rheum. 65 https://doi.org/10.1002/art.34646.
- Franklin, K.B.J., Paxinos, G., 2013. Paxinos and Franklin's The mouse brain in stereotaxic coordinates, Fourth edition. ed. Academic Press, an imprint of Elsevier, Amsterdam.
- Gallagher, D., Siddiqui, F., Fish, J., Charlat, M., Chaudry, E., Moolla, S., Gauthier-Fisher, A., Librach, C., 2019. Mesenchymal Stromal Cells Modulate Peripheral Stress-Induced Innate Immune Activation Indirectly Limiting the Emergence of Neuroinflammation-Driven Depressive and Anxiety-like Behaviors. Biol. Psychiatry 86. 712–724. https://doi.org/10.1016/j.bionsych.2019.07.015.
- 86, 712–724. https://doi.org/10.1016/j.biopsych.2019.07.015.
 Gellner, A.K., Sitter, A., Rackiewicz, M., Sylvester, M., Philipsen, A., Zimmer, A., Stein, V., 2022. Stress vulnerability shapes disruption of motor cortical neuroplasticity.
 Translational Psychiatry 2022 12:1 12, 1–13. https://doi.org/10.1038/s41398-022-01855-8.
- Geraghty, T., Winter, D.R., Miller, R.J., Miller, R.E., Malfait, A.-M., 2021. Neuroimmune interactions and osteoarthritis pain: focus on macrophages. Pain Rep 6, e892.
- Geyer, M., Schönfeld, C., 2018. Novel Insights into the Pathogenesis of Osteoarthritis. Curr. Rheumatol. Rev. 14, 98–107.
- Ghasemlou, N., Chiu, I.M., Julien, J.-P., Woolf, C.J., 2015. CD11b+Ly6G- myeloid cells mediate mechanical inflammatory pain hypersensitivity. PNAS 112, E6808–E6817. https://doi.org/10.1073/pnas.1501372112.
- Glasson, S.S., Chambers, M.G., Van Den Berg, W.B., Little, C.B., 2010. The OARSI histopathology initiative recommendations for histological assessments of osteoarthritis in the mouse. Osteoarthr. Cartil. 18, S17–S23. https://doi.org/10.1016/j.joca.2010.05.025.
- Golden, S.A., Covington, H.E., Berton, O., Russo, S.J., 2011. A standardized protocol for repeated social defeat stress in mice. Nat. Protoc. 6, 1183–1191. https://doi.org/ 10.1038/nprot.2011.361.
- Greenwood, B.N., Fleshner, M., 2019. Voluntary wheel running: a useful rodent model for investigating mechanisms of stress robustness and exercise motivation. Current Opinion in Behavioral Sciences, Psychoneuroimmunology 28, 78–84. https://doi. org/10.1016/j.cobeha.2019.02.001.
- Haraden, C.A., Huebner, J.L., Hsueh, M.F., Li, Y.J., Kraus, V.B., 2019. Synovial fluid biomarkers associated with osteoarthritis severity reflect macrophage and neutrophil related inflammation. Arthritis Res. Ther. 21, 146. https://doi.org/10.1186/s13075-019.1023 x
- Harris, A.Z., Atsak, P., Bretton, Z.H., Holt, E.S., Alam, R., Morton, M.P., Abbas, A.I., Leonardo, E.D., Bolkan, S.S., Hen, R., Gordon, J.A., 2018. A Novel Method for

- Chronic Social Defeat Stress in Female Mice. Neuropsychopharmacol. 43, 1276-1283. https://doi.org/10.1038/npp.2017.259.
- Harsanyi, S., Kupcova, I., Danisovic, L., Klein, M., 2023. Selected Biomarkers of Depression: What Are the Effects of Cytokines and Inflammation? Int. J. Mol. Sci. 24, 578. https://doi.org/10.3390/ijms24010578.
- Harth, M., Nielson, W.R., 2019. Pain and affective distress in arthritis: relationship to immunity and inflammation. Expert Rev. Clin. Immunol. 15, 541–552. https://doi. org/10.1080/1744666X.2019.1573675.
- He, Y., Wang, Y., Yu, H., Tian, Y., Chen, X., Chen, C., et al., 2023. Protective effect of Nr4a2 (Nurr1) against LPS-induced depressive-like behaviors via regulating activity of microglia and CamkII neurons in anterior cingulate cortex. Pharmacological Research 191, 106717.
- Himmerich, H., Patsalos, O., Lichtblau, N., Ibrahim, M.A.A., Dalton, B., 2019. Cytokine Research in Depression: Principles, Challenges, and Open Questions. Frontiers. Psychiatry 10.
- Hodes, G.E., Pfau, M.L., Leboeuf, M., Golden, S.A., Christoffel, D.J., Bregman, D., Rebusi, N., Heshmati, M., Aleyasin, H., Warren, B.L., Lebonté, B., Horn, S., Lapidus, K.A., Stelzhammer, V., Wong, E.H.F., Bahn, S., Krishnan, V., Bolaños-Guzman, C.A., Murrough, J.W., Merad, M., Russo, S.J., 2014. Individual differences in the peripheral immune system promote resilience versus susceptibility to social stress. PNAS 111, 16136–16141. https://doi.org/10.1073/pnas.1415191111.
- Hsueh, M., Zhang, X., Wellman, S.S., Bolognesi, M.P., Kraus, V.B., 2021. Synergistic Roles of Macrophages and Neutrophils in Osteoarthritis Progression. Arthritis Rheumatol. 73, 89–99. https://doi.org/10.1002/art.41486.
- Hunter, D.J., Bierma-Zeinstra, S., 2019. Osteoarthritis. Lancet 393, 1745–1759. https://doi.org/10.1016/S0140-6736(19)30417-9.
- Imbe, H., Kimura, A., 2015. Repeated forced swim stress prior to complete Freund's adjuvant injection enhances mechanical hyperalgesia and attenuates the expression of pCREB and ΔFosB and the acetylation of histone H3 in the insular cortex of rat. Neuroscience 301, 12–25.
- Ishikawa, Y., Kitaoka, S., Kawano, Y., Ishii, S., Suzuki, T., Wakahashi, K., Kato, T., Katayama, Y., Furuyashiki, T., 2020. Repeated social defeat stress induces neutrophil mobilization in mice: maintenance after cessation of stress and strain-dependent difference. Br. J. Pharmacol. 1–18 https://doi.org/10.1111/bph.15203.
- Jafarzadeh, A., Nemati, M., Chauhan, P., Patidar, A., Sarkar, A., Sharifi, I., Saha, B., 2020. Interleukin-27 Functional Duality Balances Leishmania Infectivity and Pathogenesis. Front. Immunol. 11.
- Johnson, A.J., Terry, E., Bartley, E.J., Garvan, C., Cruz-Almeida, Y., Goodin, B., Glover, T.L., Staud, R., Bradley, L.A., Fillingim, R.B., Sibille, K.T., 2019. Resilience factors may buffer cellular aging in individuals with and without chronic knee pain. Mol. Pain 15. https://doi.org/10.1177/1744806919842962.
- Kim, J.-R., Kim, H.A., 2020. Molecular Mechanisms of Sex-Related Differences in Arthritis and Associated Pain. Int. J. Mol. Sci. 21, 7938. https://doi.org/10.3390/ ijms21217938.
- Kim, J., Suh, Y.H., Chang, K.A., 2021. Interleukin-17 induced by cumulative mild stress promoted depression-like behaviors in young adult mice. Mol. Brain 14, 11. https:// doi.org/10.1186/s13041-020-00726-x.
- Kong, Y., He, G., Zhang, X., Li, J., 2021. The Role of Neutrophil Extracellular Traps in Lipopolysaccharide-Induced Depression-like Behaviors in Mice. Brain Sci. 11, 1514. https://doi.org/10.3390/brainsci11111514.
- Krishnan, V., Han, M.H., Graham, D.L., Berton, O., Renthal, W., Russo, S.J., LaPlant, Q., Graham, A., Lutter, M., Lagace, D.C., Ghose, S., Reister, R., Tannous, P., Green, T.A., Neve, R.L., Chakravarty, S., Kumar, A., Eisch, A.J., Self, D.W., Lee, F.S., Tamminga, C.A., Cooper, D.C., Gershenfeld, H.K., Nestler, E.J., 2007. Molecular Adaptations Underlying Susceptibility and Resistance to Social Defeat in Brain Reward Regions. Cell 131, 391–404. https://doi.org/10.1016/j.cell.2007.09.018.
- Kummer, K.K., Mitrić, M., Kalpachidou, T., Kress, M., 2020. The Medial Prefrontal Cortex as a Central Hub for Mental Comorbidities Associated with Chronic Pain. Int. J. Mol. Sci. 21, 3440. https://doi.org/10.3390/ijms21103440.
- La Porta, C., Tappe-Theodor, A., 2020. Differential impact of psychological and psychophysical stress on low back pain in mice. Pain 161, 1442. https://doi.org/ 10.1097/j.pain.0000000000001850.
- Lehmann, M.L., Mustafa, T., Eiden, A.M., Herkenham, M., Eiden, L.E., 2013. PACAP-deficient mice show attenuated corticosterone secretion and fail to develop depressive behavior during chronic social defeat stress. Psychoneuroendocrinology 38, 702–715. https://doi.org/10.1016/j.psyneuen.2012.09.006.
- Lehmann, M.L., Samuels, J.D., Kigar, S.L., Poffenberger, C.N., Lotstein, M.L., Herkenham, M., 2022. CCR2 monocytes repair cerebrovascular damage caused by chronic social defeat stress. Brain Behav. Immun. 101, 346–358. https://doi.org/ 10.1016/j.bbi.2022.01.011.
- Lewis, J.S., Hembree, W.C., Furman, B.D., Tippets, L., Cattel, D., Huebner, J.L., Little, D., DeFrate, L.E., Kraus, V.B., Guilak, F., Olson, S.A., 2011. Acute joint pathology and synovial inflammation is associated with increased intra-articular fracture severity in the mouse knee. Osteoarthr. Cartil. 19, 864–873. https://doi.org/10.1016/j.joca.2011.04.011.
- Li, M.X., Li, Q., Sun, X.J., Luo, C., Li, Y., Wang, Y.N., Chen, J., Gong, C.Z., Li, Y.J., Shi, L. P., Zheng, Y.F., Li, R.C., Huang, X.L., Xiong, Q.J., Chen, H., 2019. Increased Homer1-mGluR5 mediates chronic stress-induced depressive-like behaviors and glutamatergic dysregulation via activation of PERK-eIF2α. Prog. Neuropsychopharmacol. Biol. Psychiatry 95, 109682. https://doi.org/10.1016/j.pnpbp.2019.109682.
- Mack, M., Cihak, J., Simonis, C., Luckow, B., Proudfoot, A.E.I., Plachý, J., Brühl, H., Frink, M., Anders, H.-J., Vielhauer, V., Pfirstinger, J., Stangassinger, M., Schlöndorff, D., 2001. Expression and Characterization of the Chemokine Receptors CCR2 and CCR5 in Mice1. J. Immunol. 166, 4697–4704. https://doi.org/10.4049/ jimmunol.166.7.4697.

- Malange, K.F., Navia-Pelaez, J.M., Dias, E.V., Lemes, J.B.P., Choi, S.-H., Dos Santos, G.G., Yaksh, T.L., Corr, M., 2022. Macrophages and glial cells: Innate immune drivers of inflammatory arthritic pain perception from peripheral joints to the central nervous system. Front. Pain Res. 3, 1018800. https://doi.org/10.3389/fpain.2022.1018800.
- Mathiessen, A., Conaghan, P.G., 2017. Synovitis in osteoarthritis: current understanding with therapeutic implications. Arthritis Res. Ther. 19, 18. https://doi.org/10.1186/ s13075-017-1229-9.
- McInnes, I.B., Schett, G., 2007. Cytokines in the pathogenesis of rheumatoid arthritis. Nat. Rev. Immunol. 7, 429–442. https://doi.org/10.1038/nri2094.
- McKim, D.B., Weber, M.D., Niraula, A., Sawicki, C.M., Liu, X., Jarrett, B.L., Ramirez-Chan, K., Wang, Y., Roeth, R.M., Sucaldito, A.D., Sobol, C.G., Quan, N., Sheridan, J. F., Godbout, J.P., 2018. Microglial recruitment of IL-1β-producing monocytes to brain endothelium causes stress-induced anxiety. Mol. Psychiatry 23, 1421–1431. https://doi.org/10.1038/mp.2017.64.
- Menard, C., Pfau, M.L., Hodes, G.E., Kana, V., Wang, V.X., Bouchard, S., Takahashi, A., Flanigan, M.E., Aleyasin, H., Leclair, K.B., Janssen, W.G., Labonté, B., Parise, E.M., Lorsch, Z.S., Golden, S.A., Heshmati, M., Tamminga, C., Turecki, G., Campbell, M., Fayad, Z.A., Tang, C.Y., Merad, M., Russo, S.J., 2017. Social stress induces neurovascular pathology promoting depression. Nat. Neurosci. 20, 1752–1760. https://doi.org/10.1038/s41593-017-0010-3.
- Molnar, V., Matišić, V., Kodvanj, I., Bjelica, R., Jeleč, Ž., Hudetz, D., Rod, E., Čukelj, F., Vrdoljak, T., Vidović, D., Starešinić, M., Sabalić, S., Dobričić, B., Petrović, T., Antičević, D., Borić, I., Košir, R., Zmrzljak, U.P., Primorac, D., 2021. Cytokines and Chemokines Involved in Osteoarthritis Pathogenesis. Int. J. Mol. Sci. 22, 9208. https://doi.org/10.3390/jims22179208.
- Mul, J.D., Soto, M., Cahill, M.E., Ryan, R.E., Takahashi, H., So, K., Zheng, J., Croote, D.E., Hirshman, M.F., La Fleur, S.E., Nestler, E.J., Goodyear, L.J., 2018. Voluntary wheel running promotes resilience to chronic social defeat stress in mice: A role for nucleus accumbens ΔfosB. Neuropsychopharmacology 43, 1934–1942. https://doi.org/ 10.1038/s41386-018-0103-z.
- Murra, D., Hilde, K.L., Fitzpatrick, A., Maras, P.M., Watson, S.J., Akil, H., 2022. Characterizing the behavioral and neuroendocrine features of susceptibility and resilience to social stress. Neurobiol. Stress 17, 100437. https://doi.org/10.1016/j. ynstr.2022.100437.
- Musich, S., Wang, S.S., Slindee, L., Kraemer, S., Yeh, C.S., 2019. Association of Resilience and Social Networks with Pain Outcomes Among Older Adults. Popul. Health Manag. 22, 511–521. https://doi.org/10.1089/pop.2018.0199.
- Nasca, C., Menard, C., Hodes, G., Bigio, B., Pena, C., Lorsch, Z., Zelli, D., Ferris, A., Kana, V., Purushothaman, I., Dobbin, J., Nassim, M., DeAngelis, P., Merad, M., Rasgon, N., Meaney, M., Nestler, E.J., McEwen, B.S., Russo, S.J., 2019.
 Multidimensional Predictors of Susceptibility and Resilience to Social Defeat Stress.
 Biol. Psychiatry 86, 483–491. https://doi.org/10.1016/j.biopsych.2019.06.030.
- Nees, T.A., Wang, N., Adamek, P., Zeitzschel, N., Verkest, C., La Porta, C., Schaefer, I., Virnich, J., Balkaya, S., Prato, V., Morelli, C., Begay, V., Lee, Y.J., Tappe-Theodor, A., Lewin, G.R., Heppenstall, P.A., Taberner, F.J., Lechner, S.G., 2023. Role of TMEM100 in mechanically insensitive nociceptor un-silencing. Nat. Commun. 14, 1899. https://doi.org/10.1038/s41467-023-37602-w.
- Neugebauer, V., 2007. Arthritis Model, Kaolin-Carrageenan Induced Arthritis (Knee). Encyclopedia of Pain 115–118. https://doi.org/10.1007/978-3-540-29805-2_283.
 Neugebauer, V., Han, J.S., Adwanikar, H., Fu, Y., Ji, G., 2007. Techniques for assessing
- Neugebauer, V., Han, J.S., Adwanikar, H., Fu, Y., Ji, G., 2007. Techniques for assessing knee joint pain in arthritis. Mol. Pain 3, 1–13. https://doi.org/10.1186/1744-8069-3-8
- Nicolaides, N.C., Kyratzi, E., Lamprokostopoulou, A., Chrousos, G.P., Charmandari, E., 2014. Stress, the Stress System and the Role of Glucocorticoids. Neuroimmunomodulation 22, 6–19. https://doi.org/10.1159/000362736.
- Nie, X., Kitaoka, S., Tanaka, K., Segi-Nishida, E., Imoto, Y., Ogawa, A., Nakano, F., Tomohiro, A., Nakayama, K., Taniguchi, M., Mimori-Kiyosue, Y., Kakizuka, A., Narumiya, S., Furuyashiki, T., 2018. The Innate Immune Receptors TLR2/4 Mediate Repeated Social Defeat Stress-Induced Social Avoidance through Prefrontal Microglial Activation. Neuron 99, 464–479.e7. https://doi.org/10.1016/j.neuron.2018.06.035
- Niraula, A., Wang, Y., Godbout, J.P., Sheridan, J.F., 2018. Corticosterone production during repeated social defeat causes monocyte mobilization from the bone marrow, glucocorticoid resistance, and neurovascular adhesion molecule expression. J. Neurosci. 38, 2328–2340. https://doi.org/10.1523/JNEUROSCI.2568-17.2018.
- Okamura, H., Yasugaki, S., Suzuki-Abe, H., Arai, Y., Sakurai, K., Yanagisawa, M., Takizawa, H., Hayashi, Y., 2022. Long-Term Effects of Repeated Social Defeat Stress on Brain Activity during Social Interaction in BALB/c Mice. eNeuro 9. https://doi.org/10.1523/ENEURO.0068-22.2022.
- Oyster, N., 1980. Changes in plasma eosinophils and cortisol of women in competition. Med Sci Sports Exerc 12, 148–152.
- Pagliusi, M.O.F., Bonet, I.J.M., Dias, E.V., Vieira, A.S., Tambeli, C.H., Parada, C.A., Sartori, C.R., 2018. Social defeat stress induces hyperalgesia and increases truncated BDNF isoforms in the nucleus accumbens regardless of the depressive-like behavior induction in mice. Eur. J. Neurosci. 48, 1635–1646. https://doi.org/10.1111/ ein.13994.
- Pagliusi, M., Bonet, I.J.M., Brandão, A.F., Magalhães, S.F., Tambeli, C.H., Parada, C.A., Sartori, C.R., 2020a. Therapeutic and Preventive Effect of Voluntary Running Wheel Exercise on Social Defeat Stress (SDS)-induced Depressive-like Behavior and Chronic Pain in Mice. Neuroscience 428, 165–177. https://doi.org/10.1016/j. neuroscience.2019.12.037.
- Pagliusi, M., Bonet, I.J.M., Lemes, J.B.P., Oliveira, A.L.L., Carvalho, N.S., Tambeli, C.H., Parada, C.A., Sartori, C.R., 2020b. Social defeat stress-induced hyperalgesia is mediated by nav 1.8+ nociceptive fibers. Neurosci. Lett. 729, 135006 https://doi. org/10.1016/j.neulet.2020.135006.

- Pfau, M.L., Menard, C., Cathomas, F., Desland, F., Kana, V., Chan, K.L., Shimo, Y., LeClair, K., Flanigan, M.E., Aleyasin, H., Walker, D.M., Bouchard, S., Mack, M., Hodes, G.E., Merad, M.M., Russo, S.J., 2019. Role of Monocyte-Derived MicroRNA106b~25 in Resilience to Social Stress. Biol. Psychiatry 86, 474–482. https://doi.org/10.1016/j.biopsych.2019.02.023.
- Piardi, L.N., Pagliusi, M., Bonet, I.J.M., Brandão, A.F., Magalhães, S.F., Zanelatto, F.B., Tambeli, C.H., Parada, C.A., Sartori, C.R., 2020. Social stress as a trigger for depressive-like behavior and persistent hyperalgesia in mice: study of the comorbidity between depression and chronic pain. J. Affect. Disord. 274, 759–767. https://doi.org/10.1016/j.jad.2020.05.144.
- Pitzer, C., Kuner, R., Tappe-Theodor, A., 2016. Voluntary and evoked behavioral correlates in inflammatory pain conditions under different social housing conditions. Pain Rep. 1, e564
- Pope, R.M., Shahrara, S., 2013. Possible roles of IL-12-family cytokines in rheumatoid arthritis. Nat. Rev. Rheumatol. 9, 252–256. https://doi.org/10.1038/ nrrheum.2012.170.
- Raghu, H., Lepus, C.M., Wang, Q., Wong, H.H., Lingampalli, N., Oliviero, F., Punzi, L., Giori, N.J., Goodman, S.B., Chu, C.R., Sokolove, J.B., Robinson, W.H., 2017. CCL2/ CCR2, but not CCL5/CCR5, mediates monocyte recruitment, inflammation and cartilage destruction in osteoarthritis. Ann. Rheum. Dis. 76, 914–922. https://doi. org/10.1136/annrheumdis-2016-210426.
- Raison, C.L., Capuron, L., Miller, A.H., 2006. Cytokines sing the blues: inflammation and the pathogenesis of depression. Trends Immunol. 27, 24–31. https://doi.org/ 10.1016/j.it.2005.11.006.
- Sawicki, C.M., Kim, J.K., Weber, M.D., Jarrett, B.L., Godbout, J.P., Sheridan, J.F., Humeidan, M., 2018. Ropivacaine and Bupivacaine prevent increased pain sensitivity without altering neuroimmune activation following repeated social defeat stress. Brain Behav. Immun. 69, 113–123. https://doi.org/10.1016/j. bbi.2017.11.005.
- Sawicki, C.M., Kim, J.K., Weber, M.D., Faw, T.D., McKim, D.B., Madalena, K.M., Lerch, J. K., Basso, D.M., Humeidan, M.L., Godbout, J.P., Sheridan, J.F., 2019. Microglia promote increased pain behavior through enhanced inflammation in the spinal cord during repeated social defeat stress. J. Neurosci. 39, 1139–1149. https://doi.org/10.1523/JNEUROSCI.2785-18.2018.
- Sawicki, C.M., Humeidan, M.L., Sheridan, J.F., 2020. Neuroimmune Interactions in Pain and Stress: An Interdisciplinary Approach. The Neuroscientist: a Review Journal Bringing Neurobiology, Neurology and Psychiatry 1073858420914747. https://doi.org/10.1177/1073858420914747.
- Scarpa, J.R., Fatma, M., Loh, Y.H.E., Traore, S.R., Stefan, T., Chen, T.H., Nestler, E.J., Labonté, B., 2020. Shared Transcriptional Signatures in Major Depressive Disorder and Mouse Chronic Stress Models. Biol. Psychiatry. https://doi.org/10.1016/j. biopsych.2019.12.029.
- Schmitz, N., Laverty, S., Kraus, V.B., Aigner, T., 2010. Basic methods in histopathology of joint tissues. Osteoarthr. Cartil. 18, S113–S116. https://doi.org/10.1016/j. joca.2010.05.026.
- Segelcke, D., Talbot, S.R., Palme, R., La Porta, C., Pogatzki-Zahn, E., Bleich, A., Tappe-Theodor, A., 2023. Experimenter familiarization is a crucial prerequisite for assessing behavioral outcomes and reduces stress in mice not only under chronic pain conditions. Sci. Rep. 13, 2289. https://doi.org/10.1038/s41598-023-29052-7.
- Seney, M.L., Huo, Z., Cahill, K., French, L., Puralewski, R., Zhang, J., Logan, R.W., Tseng, G., Lewis, D.A., Sibille, E., 2018. Opposite Molecular Signatures of Depression in Men and Women. Biological Psychiatry, Mechanisms of Depression and Antidepressant Treatment 84, 18–27. https://doi.org/10.1016/j. biopsych.2018.01.017.
- Senst, L., Baimoukhametova, D., Sterley, T.-L., Bains, J.S., 2016. Sexually dimorphic neuronal responses to social isolation. Elife 5, e18726.
- Serafini, R.A., Pryce, K.D., Zachariou, V., 2020. The Mesolimbic Dopamine System in Chronic Pain and Associated Affective Comorbidities. Biol. Psychiatry 87, 64–73. https://doi.org/10.1016/j.biopsych.2019.10.018.
- Serna-Rodríguez, M.F., Bernal-Vega, S., de la Barquera, J.-A.-O.-S., Camacho-Morales, A., Pérez-Maya, A.A., 2022. The role of damage associated molecular pattern molecules (DAMPs) and permeability of the blood-brain barrier in depression and neuroinflammation. J. Neuroimmunol. 371, 577951 https://doi.org/10.1016/j. inguroim 2022 577951
- Setiawan, E., Wilson, A.A., Mizrahi, R., Rusjan, P.M., Miler, L., Rajkowska, G., Suridjan, I., Kennedy, J.L., Rekkas, P.V., Houle, S., Meyer, J.H., 2015. Role of Translocator Protein Density, a Marker of Neuroinflammation, in the Brain During Major Depressive Episodes. JAMA Psychiat. 72, 268–275. https://doi.org/10.1001/ jamapsychiatry.2014.2427.
- Smolen, J.S., Steiner, G., 2003. Therapeutic strategies for rheumatoid arthritis. Nat. Rev. Drug Discov. 2, 473–488. https://doi.org/10.1038/nrd1109.
- Sorge, R.E., Mapplebeck, J.C.S., Rosen, S., Beggs, S., Taves, S., Alexander, J.K., Martin, L. J., Austin, J.-S., Sotocinal, S.G., Chen, D., Yang, M., Shi, X.Q., Huang, H., Pillon, N.J., Bilan, P.J., Tu, Y., Klip, A., Ji, R.-R., Zhang, J., Salter, M.W., Mogil, J.S., 2015. Different immune cells mediate mechanical pain hypersensitivity in male and female mice. Nat. Neurosci. 18, 1081–1083. https://doi.org/10.1038/nn.4053.
- Straub, R.H., Dhabhar, F.S., Bijlsma, J.W.J., Cutolo, M., 2005. How psychological stress via hormones and nerve fibers may exacerbate rheumatoid arthritis. Arthritis Rheum. 52, 16–26. https://doi.org/10.1002/art.20747.
- Stumhofer, J.S., Laurence, A., Wilson, E.H., Huang, E., Tato, C.M., Johnson, L.M., Villarino, A.V., Huang, Q., Yoshimura, A., Sehy, D., Saris, C.J.M., O'Shea, J.J., Hennighausen, L., Ernst, M., Hunter, C.A., 2006. Interleukin 27 negatively regulates the development of interleukin 17-producing T helper cells during chronic inflammation of the central nervous system. Nat. Immunol. 7, 937–945. https://doi.org/10.1038/nil376.

- Sturgeon, J.A., Finan, P.H., Zautra, A.J., 2016. Affective disturbance in rheumatoid arthritis: Psychological and disease-related pathways. Nat. Rev. Rheumatol. 12, 532–542. https://doi.org/10.1038/nrrheum.2016.112.
- Sturgeon, J.A., Zautra, A.J., 2010. Resilience: a new paradigm for adaptation to chronic pain. Curr. Pain Headache Rep. 14, 105–112. https://doi.org/10.1007/s11916-010-0095-9
- Süß, P., Rothe, T., Hoffmann, A., Schlachetzki, J.C.M., Winkler, J., 2020. The Joint-Brain Axis: Insights From Rheumatoid Arthritis on the Crosstalk Between Chronic Peripheral Inflammation and the Brain. Front. Immunol. 11, 3230. https://doi.org/ 10.3389/fimmu.2020.612104.
- Tappe-Theodor, A., Fu, Y., Kuner, R., Neugebauer, V., 2011. Homerla signaling in the amygdala counteracts pain-related synaptic plasticity, mGluR1 function and pain behaviors. Mol. Pain 7, 38. https://doi.org/10.1186/1744-8069-7-38.
- Torres-Platas, S.G., Cruceanu, C., Chen, G.G., Turecki, G., Mechawar, N., 2014. Evidence for increased microglial priming and macrophage recruitment in the dorsal anterior cingulate white matter of depressed suicides. Brain Behav. Immun. 42, 50–59. https://doi.org/10.1016/j.bbi.2014.05.007.
- Touma, C., Sachser, N., Möstl, E., Palme, R., 2003. Effects of sex and time of day on metabolism and excretion of corticosterone in urine and feces of mice. Gen. Comp. Endocrinol. 130, 267–278. https://doi.org/10.1016/S0016-6480(02)00620-2.
- Uhlig, T., Smedstad, L.M., Vaglum, P., Moum, T., Gérard, N., Kvien, T.K., 2000. The course of rheumatoid arthritis and predictors of psychological, physical and radiographic outcome after 5 years of follow-up. Rheumatology (Oxford) 39, 732–741. https://doi.org/10.1093/rheumatology/39.7.732.
- Valdrighi, N., Vago, J.P., Blom, A.B., Van De Loo, F.A.J., Davidson, E.N.B., 2022. Innate Immunity at the Core of Sex Differences in Osteoarthritic Pain? https://doi.org/ 10.3389/fphar.2022.881500.
- Vialou, V., Robison, A.J., Laplant, Q.C., Covington, H.E., Dietz, D.M., Ohnishi, Y.N., Mouzon, E., Rush, A.J., Watts, E.L., Wallace, D.L., İiguez, S.D., Ohnishi, Y.H., Steiner, M.A., Warren, B.L., Krishnan, V., Bolāos, C.A., Neve, R.L., Ghose, S., Berton, O., Tamminga, C.A., Nestler, E.J., 2010. ΔfosB in brain reward circuits mediates resilience to stress and antidepressant responses. Nat. Neurosci. 13, 745–752. https://doi.org/10.1038/nn.2551.
- Vialou, V., Bagot, R.C., Cahill, M.E., Ferguson, D., Robison, A.J., Dietz, D.M., Fallon, B., Mazei-Robison, M., Ku, S.M., Harrigan, E., Winstanley, C.A., Joshi, T., Feng, J., Berton, O., Nestler, E.J., 2014. Prefrontal Cortical Circuit for Depression- and Anxiety-Related Behaviors Mediated by Cholecystokinin: Role of ΔFosB. J. Neurosci. 34, 3878–3887. https://doi.org/10.1523/JNEUROSCI.1787-13.2014.
- Vos, T., Abajobir, A.A., Abate, K.H., Abbafati, C., Abbas, K.M., Abd-Allah, F., Abdulkader, R.S., Abdulle, A.M., Abebo, T.A., Abera, S.F., Aboyans, V., Abu-Raddad, L.J., Ackerman, I.N., Adamu, A.A., Adetokunboh, O., Afarideh, M., Afshin, A., Agarwal, S.K., Aggarwal, R., Agrawal, A., Agrawal, S., Ahmadieh, H. Ahmed, M.B., Aichour, M.T.E., Aichour, A.N., Aichour, I., Aiyar, S., Akinyemi, R.O., Akseer, N., Al Lami, F.H., Alahdab, F., Al-Aly, Z., Alam, K., Alam, N., Alam, T., Alasfoor, D., Alene, K.A., Ali, R., Alizadeh-Navaei, R., Alkerwi, A., Alla, F., Allebeck, P., Allen, C., Al-Maskari, F., Al-Raddadi, R., Alsharif, U., Alsowaidi, S. Altirkawi, K.A., Amare, A.T., Amini, E., Ammar, W., Amoako, Y.A., Andersen, H.H., Antonio, C.A.T., Anwari, P., Ärnlöv, J., Artaman, A., Aryal, K.K., Asayesh, H., Asgedom, S.W., Assadi, R., Atey, T.M., Atnafu, N.T., Atre, S.R., Avila-Burgos, L., Avokphako, E.F.G.A., Awasthi, A., Bacha, U., Badawi, A., Balakrishnan, K., Banerjee, A., Bannick, M.S., Barac, A., Barber, R.M., Barker-Collo, S.L., Bärnighausen, T., Barquera, S., Barregard, L., Barrero, L.H., Basu, S., Battista, B., Battle, K.E., Baune, B.T., Bazargan-Hejazi, S., Beardsley, J., Bedi, N., Beghi, E., Béjot, Y., Bekele, B.B., Bell, M.L., Bennett, D.A., Bensenor, I.M., Benson, J., Berhane, A., Berhe, D.F., Bernabé, E., Betsu, B.D., Beuran, M., Beyene, A.S., Bhala, N., Bhansali, A., Bhatt, S., Bhutta, Z.A., Biadgilign, S., Bicer, B.K., Bienhoff, K., Bikbov, B., Birungi, C., Biryukov, S., Bisanzio, D., Bizuayehu, H.M., Boneya, D.J., Boufous, S., Bourne, R.R.A., Brazinova, A., Brugha, T.S., Buchbinder, R., Bulto, L.N. B., Bumgarner, B.R., Butt, Z.A., Cahuana-Hurtado, L., Cameron, E., Car, M., Carabin, H., Carapetis, J.R., Cárdenas, R., Carpenter, D.O., Carrero, J.J., Carter, A., Carvalho, F., Casey, D.C., Caso, V., Castañeda-Orjuela, C.A., Castle, C.D., Catalá-López, F., Chang, H.-Y., Chang, J.-C., Charlson, F.J., Chen, H., Chibalabala, M., Chibueze, C.E., Chisumpa, V.H., Chitheer, A.A., Christopher, D.J., Ciobanu, L.G., Cirillo, M., Colombara, D., Cooper, C., Cortesi, P.A., Criqui, M.H., Crump, J.A., Dadi, A.F., Dalal, K., Dandona, L., Dandona, R., das Neves, J., Davitoiu, D.V., de Courten, B., De Leo, D.D., Defo, B.K., Degenhardt, L., Deiparine, S., Dellavalle, R.P., Deribe, K., Des Jarlais, D.C., Dey, S., Dharmaratne, S.D., Dhillon, P.K., Dicker, D., Ding, E.L., Djalalinia, S., Do, H.P., Dorsey, E.R., dos Santos, K.P.B., Douwes-Schultz, D., Doyle, K.E., Driscoll, T.R., Dubey, M., Duncan, B.B., El-Khatib, Z.Z., Ellerstrand, J., Enayati, A., Endries, A.Y., Ermakov, S.P., Erskine, H.E., Eshrati, B., Eskandarieh, S., Esteghamati, A., Estep, K., Fanuel, F.B.B., Farinha, C.S.E.S., Faro, A., Farzadfar, F., Fazeli, M.S., Feigin, V.L., Fereshtehnejad, S.-M., Fernandes, J.C., Ferrari, A.J., Feyissa, T.R., Filip, I., Fischer, F., Fitzmaurice, C., Flaxman, A.D., Flor, L.S., Foigt, N., Foreman, K.J., Franklin, R.C., Fullman, N., Fürst, T., Furtado, J.M., Futran, N.D., Gakidou, E., Ganji, M., Garcia-Basteiro, A.L., Gebre, T., Gebrehiwot, T.T., Geleto, A., Gemechu, B.L., Gesesew, H.A., Gething, P.W., Ghajar, A., Gibney, K.B., Gill, P.S Gillum, R.F., Ginawi, I.A.M., Giref, A.Z., Gishu, M.D., Giussani, G., Godwin, W.W., Gold, A.L., Goldberg, E.M., Gona, P.N., Goodridge, A., Gopalani, S.V., Goto, A., Goulart, A.C., Griswold, M., Gugnani, H.C., Gupta, Rahul, Gupta, Rajeev, Gupta, T., Gupta, V., Hafezi-Nejad, N., Hailu, G.B., Hailu, A.D., Hamadeh, R.R., Hamidi, S., Handal, A.J., Hankey, G.J., Hanson, S.W., Hao, Y., Harb, H.L., Hareri, H.A., Haro, J. M., Harvey, J., Hassanvand, M.S., Havmoeller, R., Hawley, C., Hay, S.I., Hay, R.J., Henry, N.J., Heredia-Pi, I.B., Hernandez, J.M., Heydarpour, P., Hoek, H.W., Hoffman, H.J., Horita, N., Hosgood, H.D., Hostiuc, S., Hotez, P.J., Hoy, D.G., Htet, A. S., Hu, G., Huang, H., Huynh, C., Iburg, K.M., Igumbor, E.U., Ikeda, C., Irvine, C.M. S., Jacobsen, K.H., Jahanmehr, N., Jakovljevic, M.B., Jassal, S.K., Javanbakht, M.,

Jayaraman, S.P., Jeemon, P., Jensen, P.N., Jha, V., Jiang, G., John, D., Johnson, S.C., Johnson, C.O., Jonas, J.B., Jürisson, M., Kabir, Z., Kadel, R., Kahsay, A., Kamal, R., Kan, H., Karam, N.E., Karch, A., Karema, C.K., Kasaeian, A., Kassa, G.M., Kassaw, N. A., Kassebaum, N.J., Kastor, A., Katikireddi, S.V., Kaul, A., Kawakami, N., Keiyoro, P. N., Kengne, A.P., Keren, A., Khader, Y.S., Khalil, I.A., Khan, E.A., Khang, Y.-H., Khosravi, A., Khubchandani, J., Kiadaliri, A.A., Kieling, C., Kim, Y.J., Kim, D., Kim, P., Kimokoti, R.W., Kinfu, Y., Kisa, A., Kissimova-Skarbek, K.A., Kivimaki, M., Knudsen, A.K., Kokubo, Y., Kolte, D., Kopec, J.A., Kosen, S., Koul, P.A., Koyanagi, A., Kravchenko, M., Krishnaswami, S., Krohn, K.J., Kumar, G.A., Kumar, P., Kumar, S., Kyu, H.H., Lal, D.K., Lalloo, R., Lambert, N., Lan, Q., Larsson, A., Lavados, P.M., Leasher, J.L., Lee, P.H., Lee, J.-T., Leigh, J., Leshargie, C.T., Leung, J., Leung, R., Levi, M., Li, Yichong, Li, Yongmei, Li Kappe, D., Liang, X., Liben, M.L., Lim, S.S., Linn, S., Liu, P.Y., Liu, A., Liu, S., Liu, Y., Lodha, R., Logroscino, G., London, S.J., Looker, K.J., Lopez, A.D., Lorkowski, S., Lotufo, P.A., Low, N., Lozano, R., Lucas, T.C. D., Macarayan, E.R.K., Magdy Abd El Razek, H., Magdy Abd El Razek, M., Mahdavi, M., Majdan, M., Majdzadeh, R., Majeed, A., Malekzadeh, R., Malhotra, R., Malta, D. C., Mamun, A.A., Manguerra, H., Manhertz, T., Mantilla, A., Mantovani, L.G., Mapoma, C.C., Marczak, L.B., Martinez-Raga, J., Martins-Melo, F.R., Martopullo, I., März, W., Mathur, M.R., Mazidi, M., McAlinden, C., McGaughey, M., McGrath, J.J., McKee, M., McNellan, C., Mehata, S., Mehndiratta, M.M., Mekonnen, T.C., Memiah, P., Memish, Z.A., Mendoza, W., Mengistie, M.A., Mengistu, D.T., Mensah, G.A., Meretoja, T.J., Meretoja, A., Mezgebe, H.B., Micha, R., Millear, A., Miller, T.R., Mills, E.J., Mirarefin, M., Mirrakhimov, E.M., Misganaw, A., Mishra, S.R., Mitchell, P.B., Mohammad, K.A., Mohammadi, A., Mohammed, K.E., Mohammed, S., Mohanty, S. K., Mokdad, A.H., Mollenkopf, S.K., Monasta, L., Montico, M., Moradi-Lakeh, M., Moraga, P., Mori, R., Morozoff, C., Morrison, S.D., Moses, M., Mountjoy-Venning, C., Mruts, K.B., Mueller, U.O., Muller, K., Murdoch, M.E., Murthy, G.V.S., Musa, K.I., Nachega, J.B., Nagel, G., Naghavi, M., Naheed, A., Naidoo, K.S., Naldi, L., Nangia, V., Natarajan, G., Negasa, D.E., Negoi, R.I., Negoi, I., Newton, C.R., Ngunjiri, J.W., Nguyen, T.H., Nguyen, Q.L., Nguyen, C.T., Nguyen, G., Nguyen, M., Nichols, E., Ningrum, D.N.A., Nolte, S., Nong, V.M., Norrving, B., Noubiap, J.J.N., O'Donnell, M. J., Ogbo, F.A., Oh, I.-H., Okoro, A., Oladimeji, O., Olagunju, T.O., Olagunju, A.T., Olsen, H.E., Olusanya, B.O., Olusanya, J.O., Ong, K., Opio, J.N., Oren, E., Ortiz, A., Osgood-Zimmerman, A., Osman, M., Owolabi, M.O., Pa, M., Pacella, R.E., Pana, A., Panda, B.K., Papachristou, C., Park, E.-K., Parry, C.D., Parsaeian, M., Patten, S.B., Patton, G.C., Paulson, K., Pearce, N., Pereira, D.M., Perico, N., Pesudovs, K., Peterson, C.B., Petzold, M., Phillips, M.R., Pigott, D.M., Pillay, J.D., Pinho, C., Plass, D., Pletcher, M.A., Popova, S., Poulton, R.G., Pourmalek, F., Prabhakaran, D., Prasad, N.M., Prasad, N., Purcell, C., Qorbani, M., Quansah, R., Quintanilla, B.P.A., Rabiee, R.H.S., Radfar, A., Rafay, A., Rahimi, K., Rahimi-Movaghar, A., Rahimi-Movaghar, V., Rahman, M.H.U., Rahman, M., Rai, R.K., Rajsic, S., Ram, U., Ranabhat, C.L., Rankin, Z., Rao, P.C., Rao, P.V., Rawaf, S., Ray, S.E., Reiner, R.C., Reinig, N., Reitsma, M.B., Remuzzi, G., Renzaho, A.M.N., Resnikoff, S., Rezaei, S., Ribeiro, A.L., Ronfani, L., Roshandel, G., Roth, G.A., Roy, A., Rubagotti, E., Ruhago, G.M., Saadat, S., Sadat, N., Safdarian, M., Safi, S., Safiri, S., Sagar, R., Sahathevan, R., Salama, J., Saleem, H.O.B., Salomon, J.A., Salvi, S.S., Samy, A.M., Sanabria, J.R., Santomauro, D., Santos, I.S., Santos, J.V., Santric Milicevic, M.M., Sartorius, B., Satpathy, M., Sawhney, M., Saxena, S., Schmidt, M.I., Schneider, I.J.C., Schöttker, B., Schwebel, D. C., Schwendicke, F., Seedat, S., Sepanlou, S.G., Servan-Mori, E.E., Setegn, T., Shackelford, K.A., Shaheen, A., Shaikh, M.A., Shamsipour, M., Shariful Islam, S.M., Sharma, J., Sharma, R., She, J., Shi, P., Shields, C., Shifa, G.T., Shigematsu, M., Shinohara, Y., Shiri, R., Shirkoohi, R., Shirude, S., Shishani, K., Shrime, M.G., Sibai, A.M., Sigfusdottir, I.D., Silva, D.A.S., Silva, J.P., Silveira, D.G.A., Singh, J.A., Singh, N.P., Sinha, D.N., Skiadaresi, E., Skirbekk, V., Slepak, E.L., Sligar, A., Smith, D.L., Smith, M., Sobaih, B.H.A., Sobngwi, E., Sorensen, R.J.D., Sousa, T.C.M., Sposato, L. A., Sreeramareddy, C.T., Srinivasan, V., Stanaway, J.D., Stathopoulou, V., Steel, N., Stein, M.B., Stein, D.J., Steiner, T.J., Steiner, C., Steinke, S., Stokes, M.A., Stovner, L. J., Strub, B., Subart, M., Sufiyan, M.B., Sunguya, B.F., Sur, P.J., Swaminathan, S., Sykes, B.L., Sylte, D.O., Tabarés-Seisdedos, R., Taffere, G.R., Takala, J.S., Tandon, N., Tavakkoli, M., Taveira, N., Taylor, H.R., Tehrani-Banihashemi, A., Tekelab, T. Terkawi, A.S., Tesfaye, D.J., Tesssema, B., Thamsuwan, O., Thomas, K.E., Thrift, A. G., Tiruye, T.Y., Tobe-Gai, R., Tollanes, M.C., Tonelli, M., Topor-Madry, R., Tortajada, M., Touvier, M., Tran, B.X., Tripathi, S., Troeger, C., Truelsen, T., Tsoi, D., Tuem, K.B., Tuzcu, E.M., Tyrovolas, S., Ukwaja, K.N., Undurraga, E.A., Uneke, C.J., Updike, R., Uthman, O.A., Uzochukwu, B.S.C., van Boven, J.F.M., Varughese, S., Vasankari, T., Venkatesh, S., Venketasubramanian, N., Vidavalur, R., Violante, F.S., Vladimirov, S.K., Vlassov, V.V., Vollset, S.E., Wadilo, F., Wakayo, T., Wang, Y.-P., Weaver, M., Weichenthal, S., Weiderpass, E., Weintraub, R.G., Werdecker, A., Westerman, R., Whiteford, H.A., Wijeratne, T., Wiysonge, C.S., Wolfe, C.D.A., Woodbrook, R., Woolf, A.D., Workicho, A., Xavier, D., Xu, G., Yadgir, S., Yaghoubi, M., Yakob, B., Yan, L.L., Yano, Y., Ye, P., Yimam, H.H., Yip, P., Yonemoto, N., Yoon, S.-J., Yotebieng, M., Younis, M.Z., Zaidi, Z., Zaki, M.E.S., Zegeye, E.A., Zenebe, Z.M., Zhang, X., Zhou, M., Zipkin, B., Zodpey, S., Zuhlke, L.J., Murray, C.J.L., 2017 Global, regional, and national incidence, prevalence, and years lived with disability for 328 diseases and injuries for 195 countries, 1990-2016: a systematic analysis for the Global Burden of Disease Study 2016. Lancet 390, 1211-1259. https://doi.org 10.1016/S0140-6736(17)32154-2

- Wang, Y., Wang, J., Liu, X., Zhu, T., 2021. Detecting Depression Through Gait Data: Examining the Contribution of Gait Features in Recognizing Depression. Frontiers in Psychiatry 12.
- Wang, H., Liu, L., Chen, X., Zhou, C., Rao, X., Li, W., Li, W., Liu, Y., Fang, L., Zhang, H., Song, J., Ji, P., Xie, P., 2022a. MicroRNA–Messenger RNA Regulatory Network Mediates Disrupted TH17 Cell Differentiation in Depression. Front. Psych. 13, 824209 https://doi.org/10.3389/fpsyt.2022.824209.
- Wang, W., Liu, W.Z., Wang, Z.L., Duan, D.X., Wang, X.Y., Liu, S.J., Wang, Z.J., Xing, G.G., Xing, Y., 2022b. Spinal microglial activation promotes perioperative social defeat

- stress-induced prolonged postoperative pain in a sex-dependent manner. Brain Behav. Immun. 100, 88–104. https://doi.org/10.1016/j.bbi.2021.11.010.
- Weber, M.D., Godbout, J.P., Sheridan, J.F., 2017. Repeated Social Defeat,
 Neuroinflammation, and Behavior: Monocytes Carry the Signal.
 Neuropsychopharmacology 42, 46–61. https://doi.org/10.1038/npp.2016.102.
- Wohleb, E.S., Powell, N.D., Godbout, J.P., Sheridan, J.F., 2013. Stress-Induced Recruitment of Bone Marrow-Derived Monocytes to the Brain Promotes Anxiety-Like Behavior. J. Neurosci. 33, 13820–13833. https://doi.org/10.1523/ JNEUROSCI.1671-13.2013.
- Wohleb, E.S., McKim, D.B., Shea, D.T., Powell, N.D., Tarr, A.J., Sheridan, J.F., Godbout, J.P., 2014. Re-establishment of Anxiety in Stress-Sensitized Mice Is Caused by Monocyte Trafficking from the Spleen to the Brain. Biological Psychiatry, Human Stem Cell Biology: New Frontier in Neurobiology of Mental Illness 75, 970–981. https://doi.org/10.1016/j.biopsych.2013.11.029.
- Wohleb, E.S., McKim, D.B., Sheridan, J.F., Godbout, J.P., 2015. Monocyte trafficking to the brain with stress and inflammation: a novel axis of immune-to-brain communication that influences mood and behavior. Front. Neurosci. 8 https://doi. org/10.3389/fnins.2014.00447.
- Wu, L., Wang, R., Zhou, Y., Zhao, D., Chen, F., Wu, X., Chen, X., Chen, S., Li, J., Zhu, J., 2022. Natural Killer Cells Infiltration in the Joints Exacerbates Collagen-Induced Arthritis. Front. Immunol. 13, 860761 https://doi.org/10.3389/ fimmu.2022.860761.

- Xu, X., Wu, K., Ma, X., Wang, W., Wang, H., Huang, M., Luo, L., Su, C., Yuan, T., Shi, H., Han, J., Wang, A., Xu, T., 2021. mGluR5-Mediated eCB Signaling in the Nucleus Accumbens Controls Vulnerability to Depressive-Like Behaviors and Pain After Chronic Social Defeat Stress. Mol. Neurobiol. 58, 4944–4958. https://doi.org/ 10.1007/s12035-021-02469-9.
- Yin, W., Gallagher, N.R., Sawicki, C.M., McKim, D.B., Godbout, J.P., Sheridan, J.F., 2019. Repeated social defeat in female mice induces anxiety-like behavior associated with enhanced myelopoiesis and increased monocyte accumulation in the brain. Brain Behav. Immun. 78, 131–142. https://doi.org/10.1016/j.bbi.2019.01.015.
- Yomogida, S., Sekiguchi, M., Konno, S., ichi, 2020. Involvement between social defeat stress and pain-related behavior in a rat lumbar disk herniation model. Eur. Spine J. 29, 2431–2440. https://doi.org/10.1007/s00586-020-06533-1.
- Yu, H., Huang, T., Lu, W.W., Tong, L., Chen, D., 2022. Osteoarthritis Pain. Int. J. Mol. Sci. 23, 4642. https://doi.org/10.3390/ijms23094642.
- Zhang, X., Wang, B., O'Callaghan, P., Hjertström, E., Jia, J., Gong, F., Zcharia, E., Nilsson, L.N.G., Lannfelt, L., Vlodavsky, I., Lindahl, U., Li, J.-P., 2012. Heparanase overexpression impairs inflammatory response and macrophage-mediated clearance of amyloid-β in murine brain. Acta Neuropathol. 124, 465–478. https://doi.org/10.1007/s00401-012-0997-1.
- Zhang, X., Wang, B., Li, J.-P., 2014. Implications of heparan sulfate and heparanase in neuroinflammation. Matrix Biol. 35, 174–181. https://doi.org/10.1016/j. matbio.2013.12.009.